



Deutsche
Gesellschaft
für Nuklearmedizin
e.V.



Translational Research in Molecular Imaging and Radionuclide Therapy

August 27 - 29, 2015

Overview Molecular Imaging PET and SPECT

**UNIKLINIK
RWTHAACHEN**
KLINIK FÜR NUKLEARMEDIZIN

F.M. Mottaghy

Medical imaging and the pathology cascade

Molecular/Cellular
disturbance



Alterations in
physiology

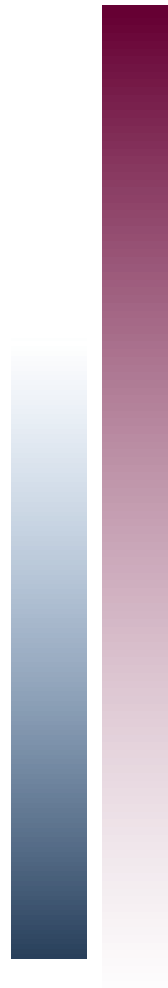


Structural
lesion

Diagnostic approach

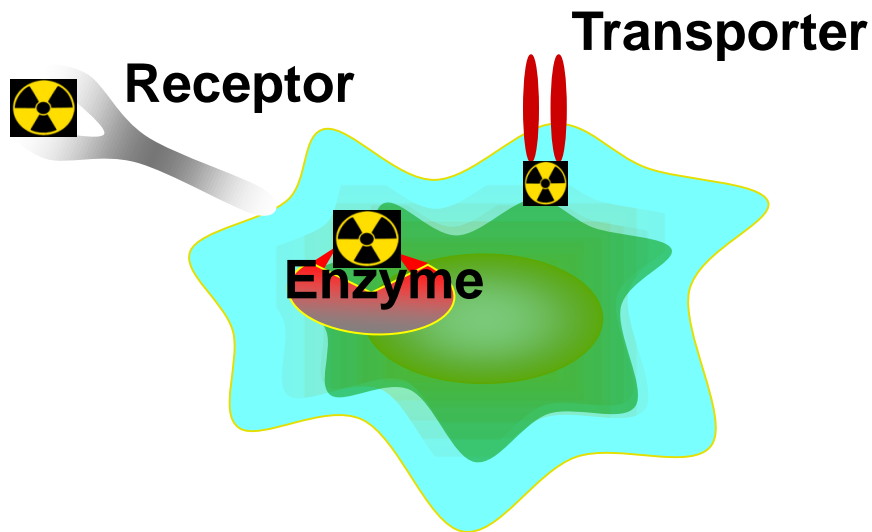
Nuclear/Molecular
Medicine

Radiology



Molecular interactions of radiolabeled probes

In vivo imaging of biological processes with radiolabeled molecular probes



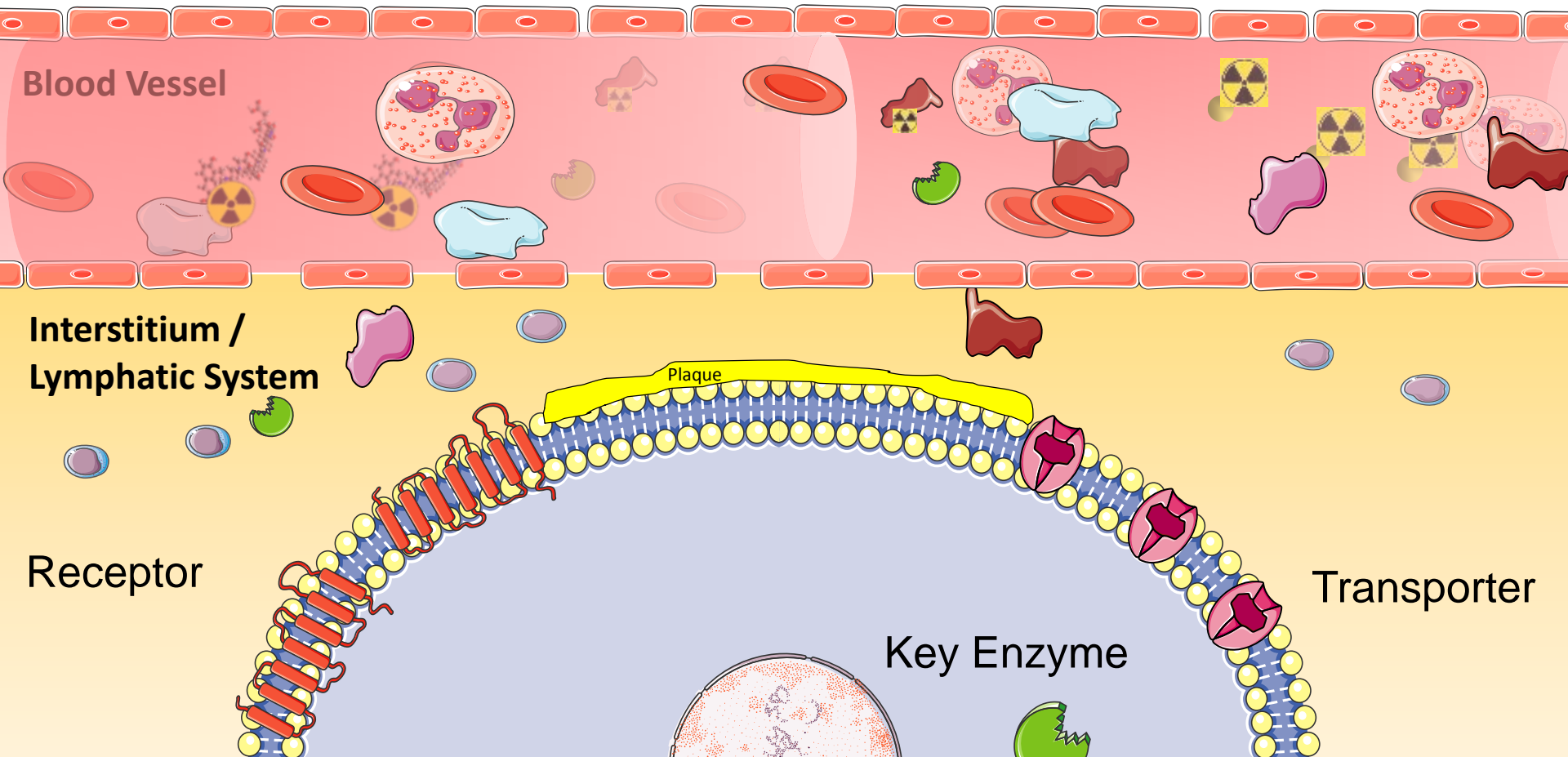
Mechanism of localization

Visualization of overexpression or increased activity of:

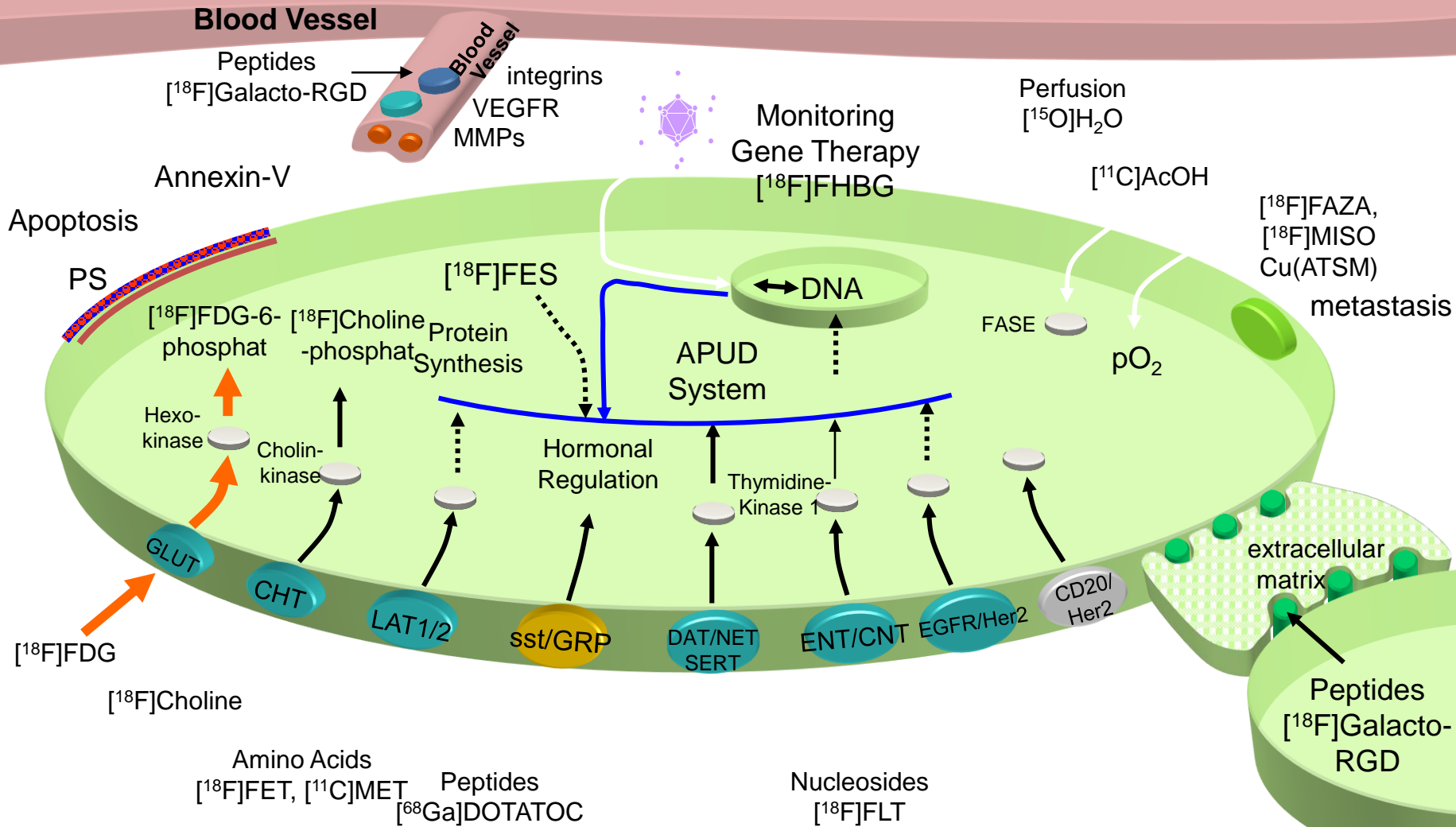
- Receptors
- Enzymes
- Transporters

Nuclear Molecular Imaging

In vivo imaging of biological processes with radiolabeled molecular probes

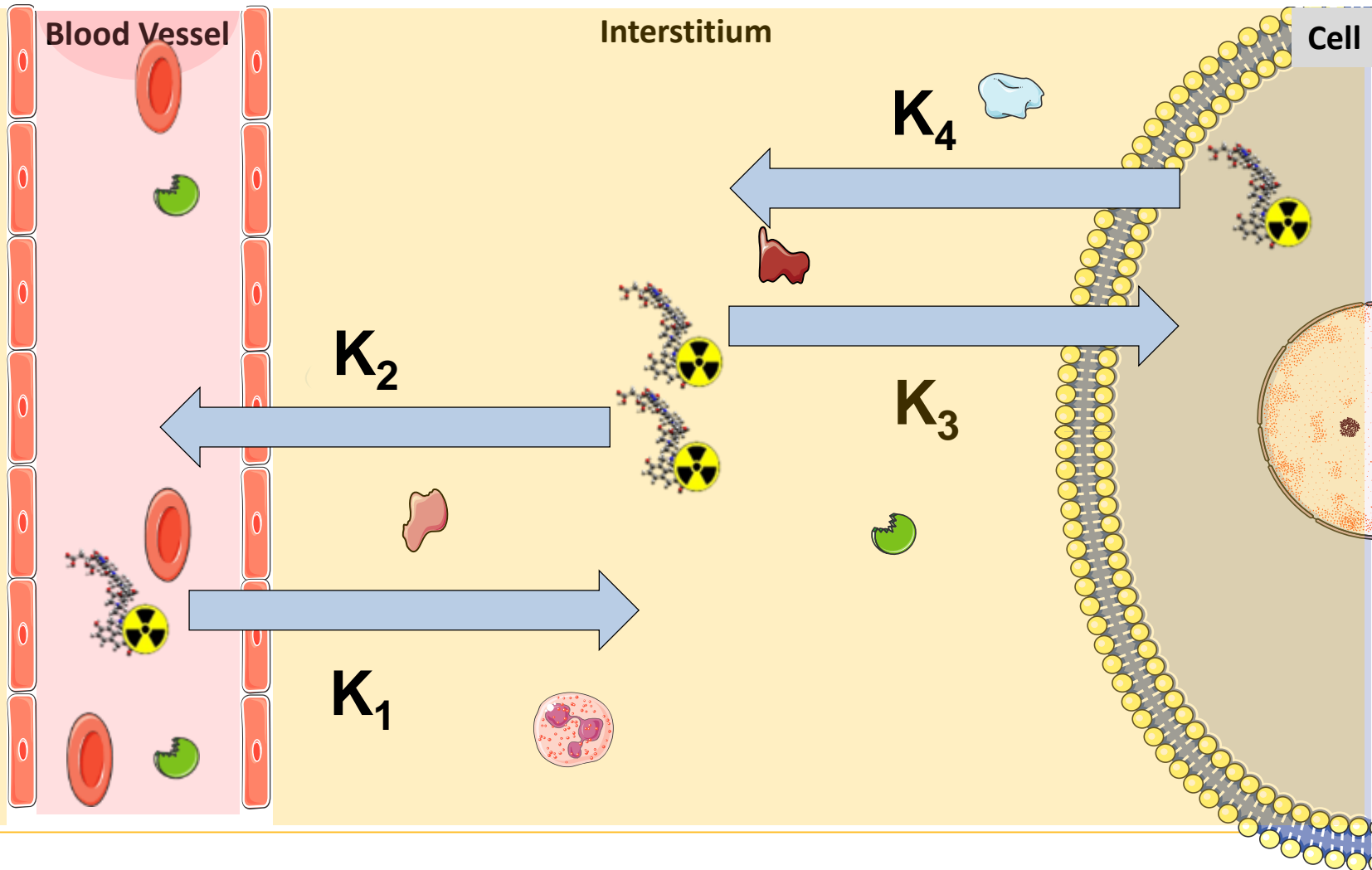


Molecular Probes (Tracers)



Wester et al., Clin Cancer Res 2007

COMPARTMENT MODEL



Steps to molecular image acquisition

1. Radionuclide



2. Synthesis of radiopharmaceutical



3. Radiopharmaceutical



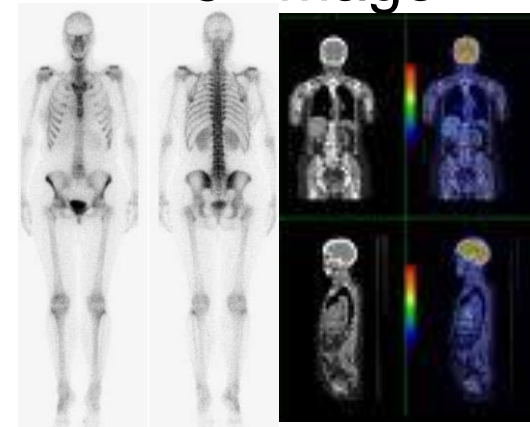
4. Application



5. Scan



6. Image



Planar Scintigraphy

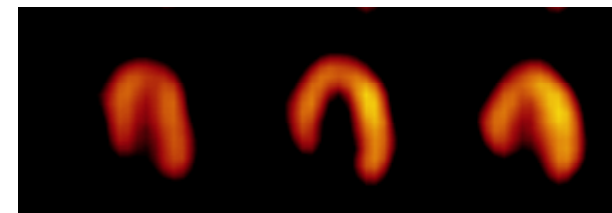
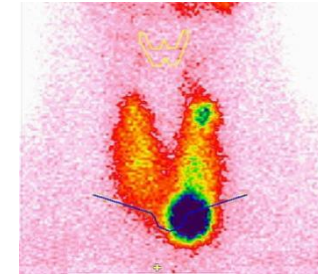
^{99m}Tc

6h HWZ
140 keV

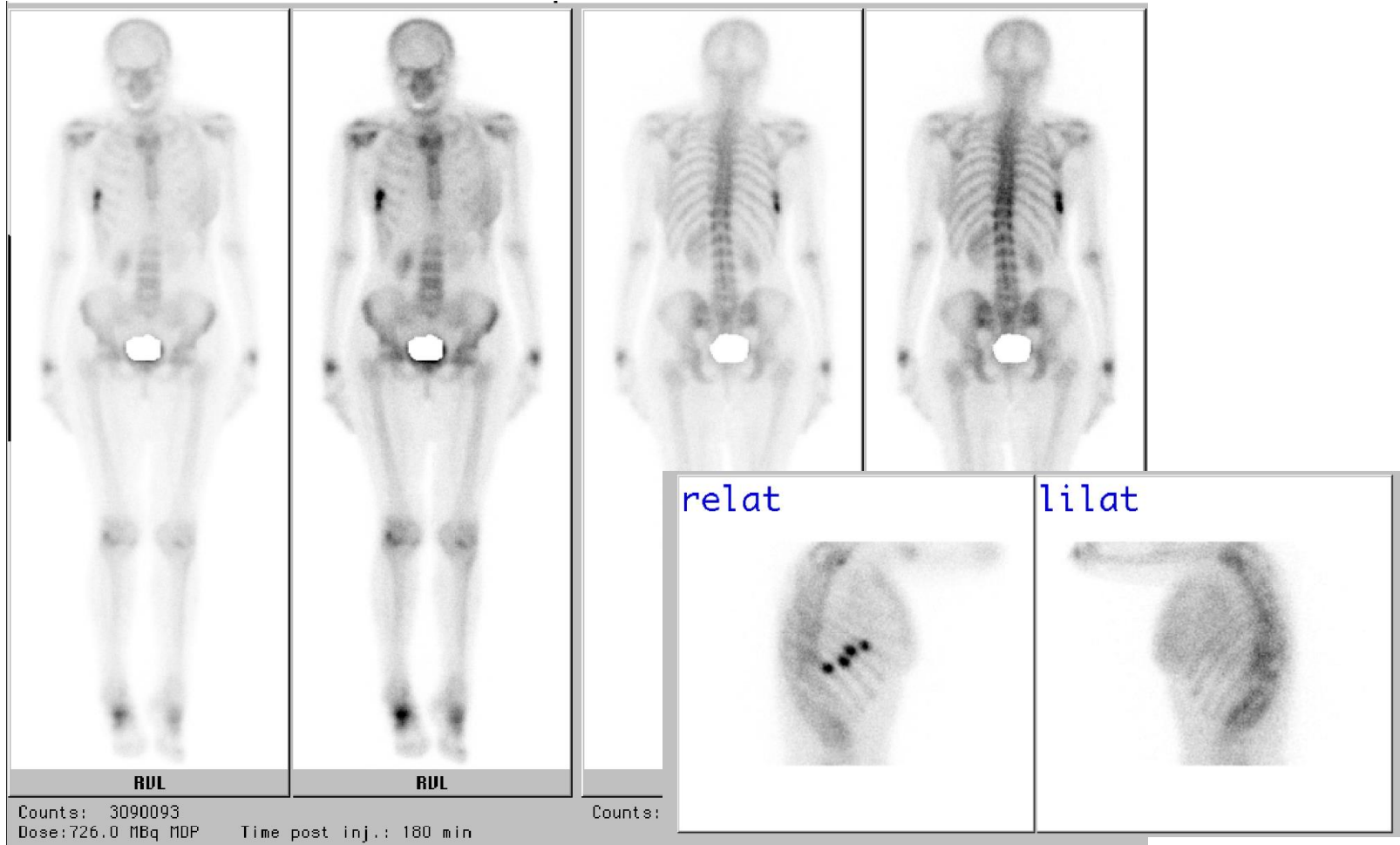
Nuklid



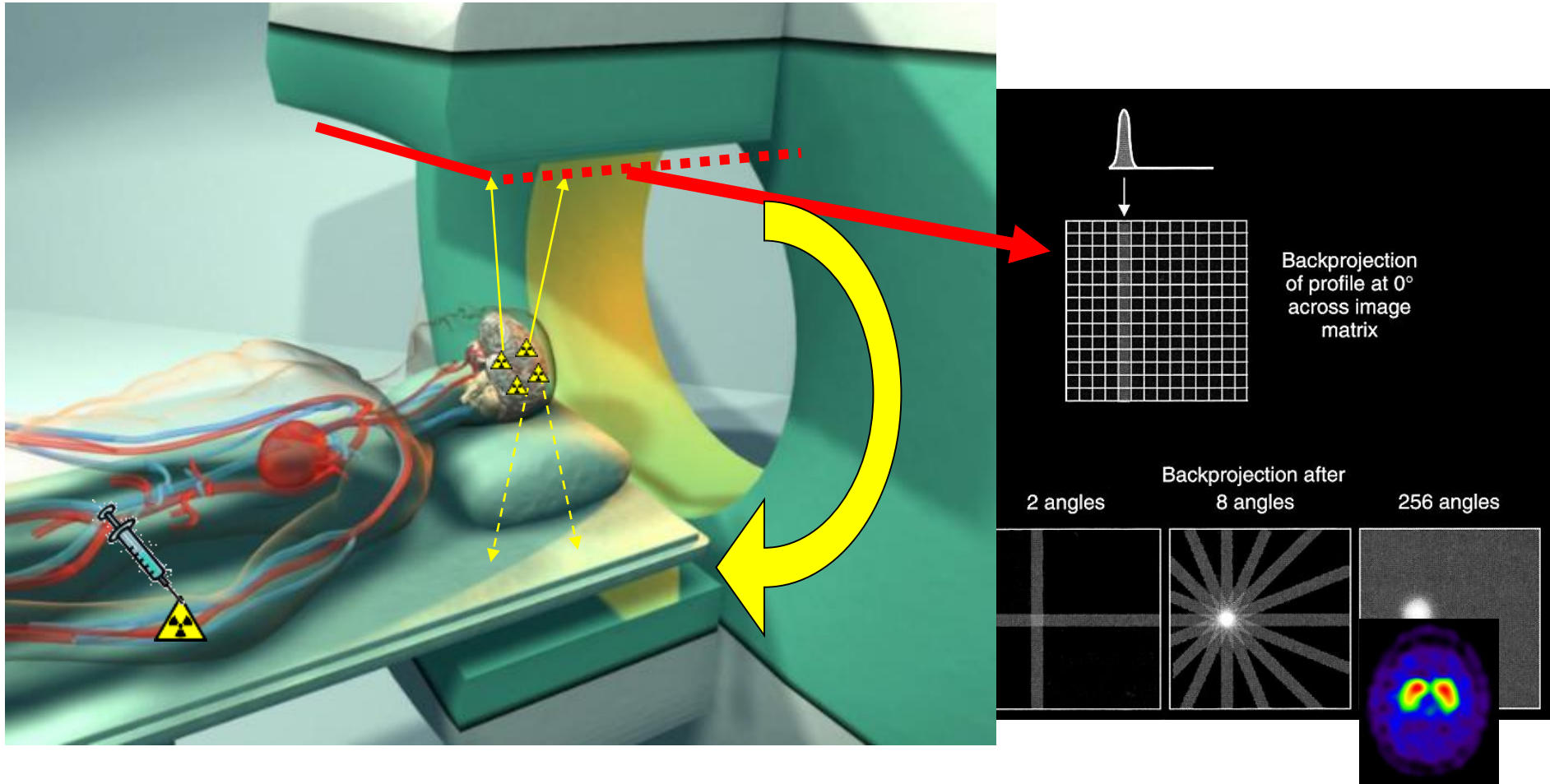
target-specific
radiopharmaceuticals



Bone-Scintigraphy (^{99m}Tc -MDP)

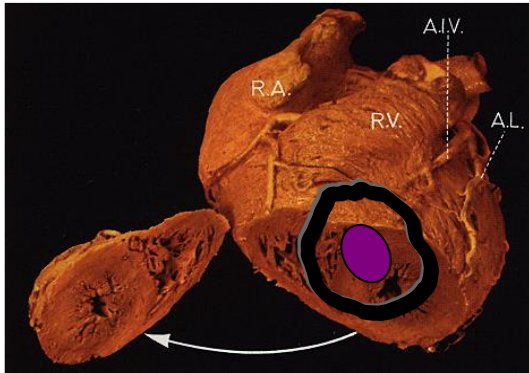


Single Photon Emission Computed Tomography (SPECT)



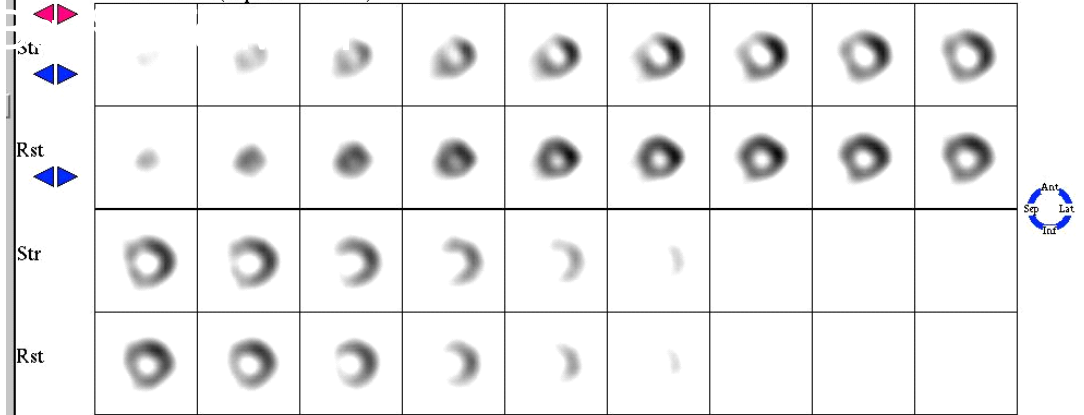
Myocardial SPECT

Cardiovascular disease, ergometry until 75 Watt



**short
axis**

Short Axis (Apex→Base)



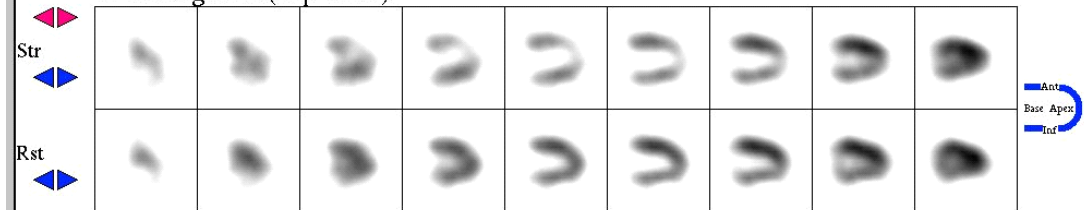
**horiz.
long
axis**

Horiz Long Axis (Post→Ant)

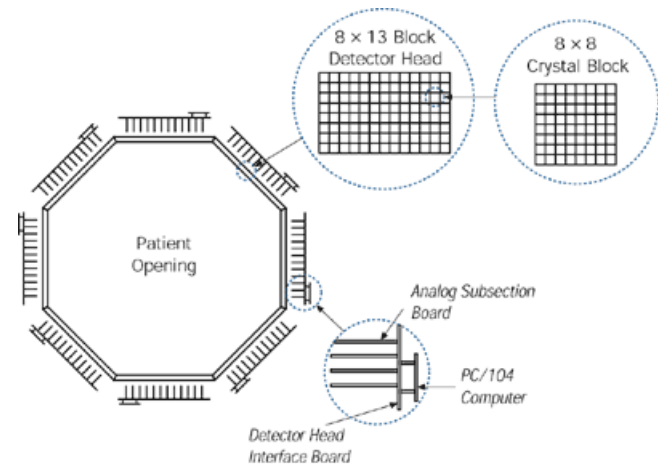
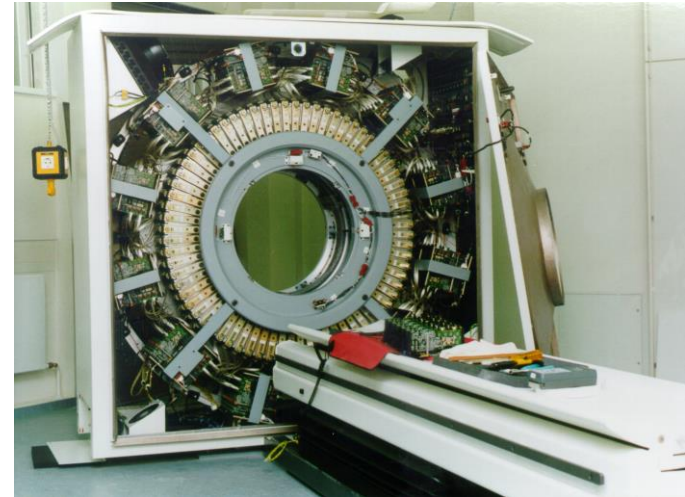


**vert.
long
axis**

Vert Long Axis (Sep→Lat)



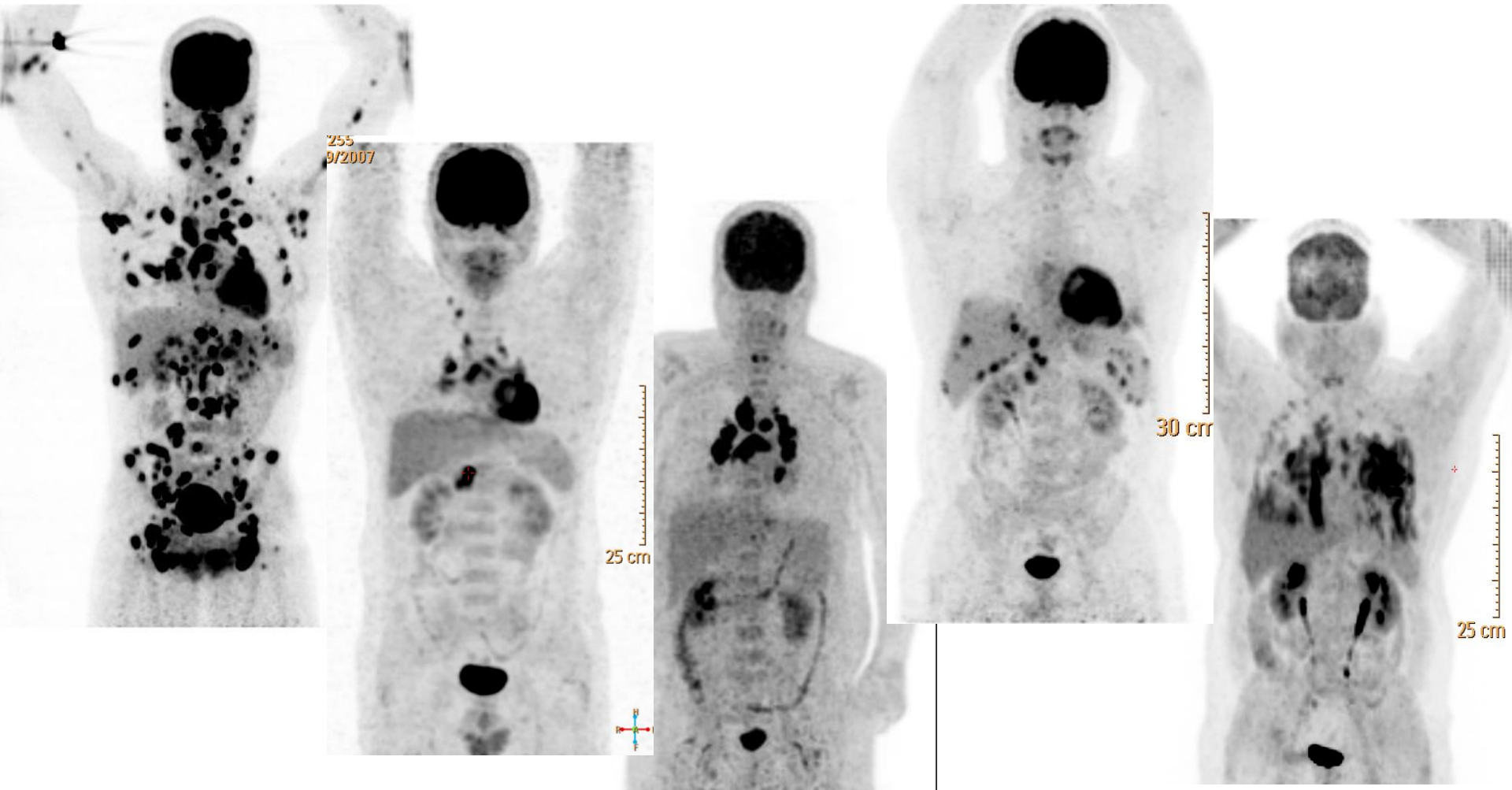
Positronen-Emissions-Tomographie (PET)

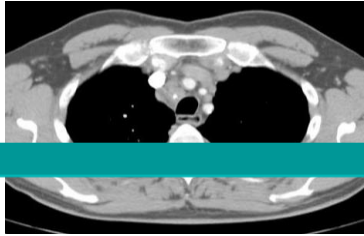
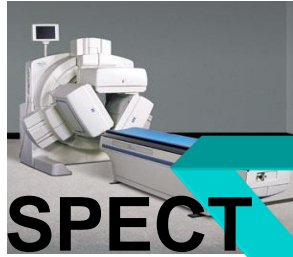


^{18}F -Fluoride PET

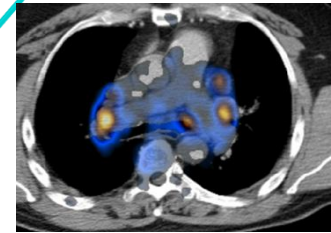


Fluorodeoxyglucose-PET (Sarkoidosis)

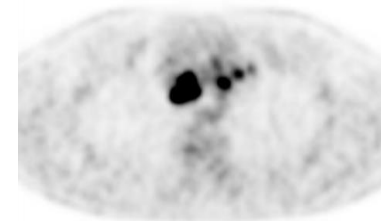




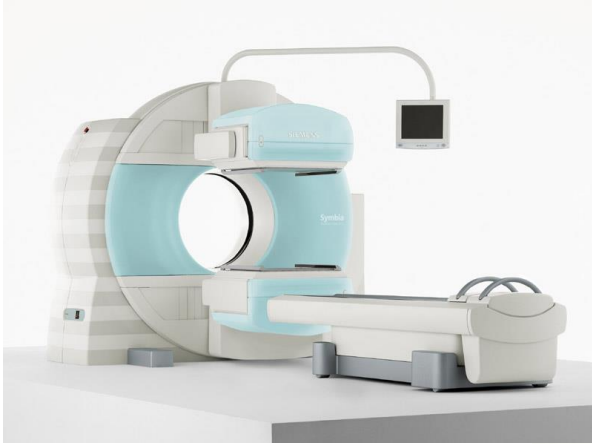
**Multimodal
molecular/functional
Imaging**



CT



SPECT/CT



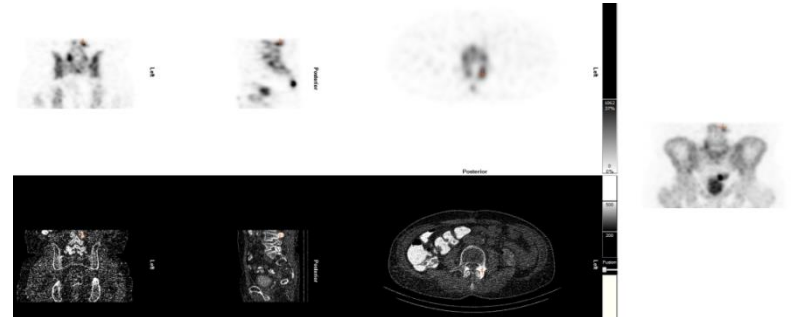
SPECT/CT Prostate Cancer Bone Scan

Staging I

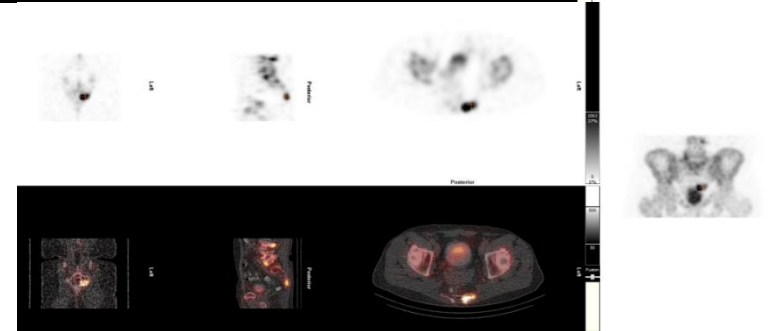


- Age 68 yrs., Post OP
- PSA increased
- Bone Scan, (745 MBq Tc-99m-HDP)
- SPECT/CT

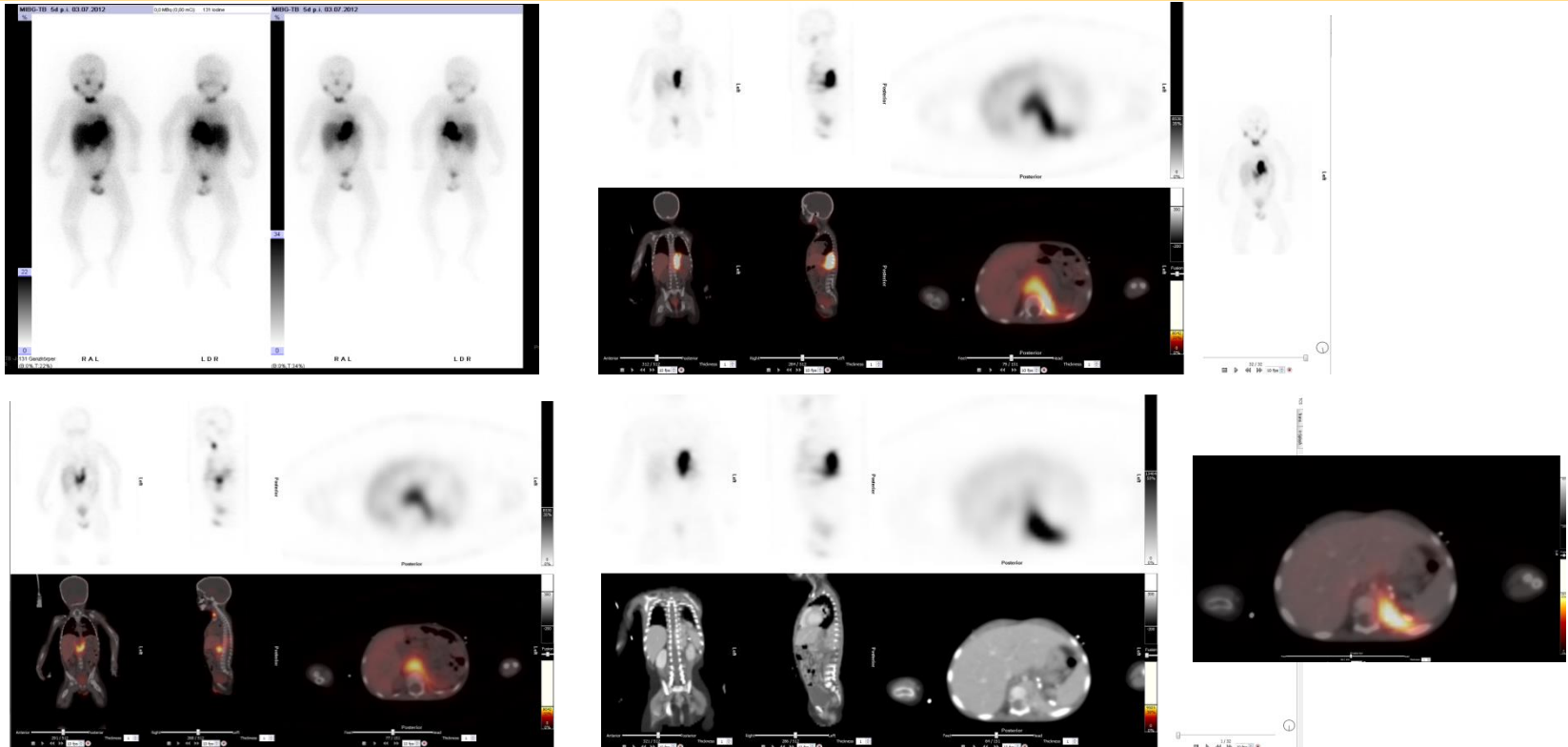
Staging II
Pedicle of vertebral arch



Staging III
Metastasis Os sacrum

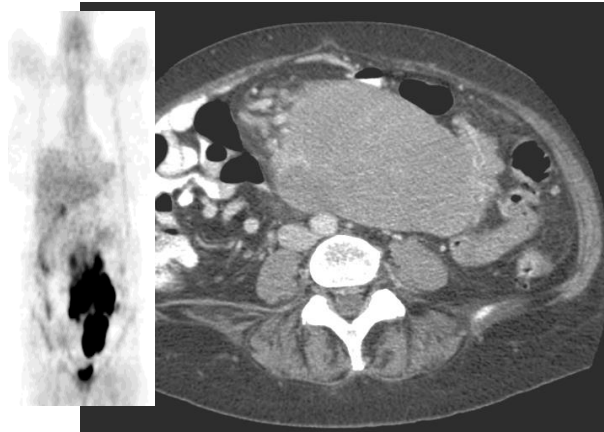


MIBG SPECT/CT

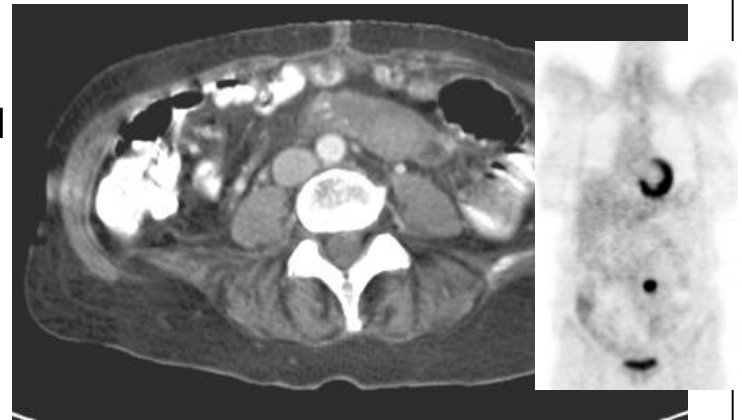


- 2 yrs., Neuroblastoma Stage IV, post therapy, Neuroblastoma recurrence with cerebral and abdominal metastases, Tumour progress under recurrence therapy
- Planar imaging and SPECT/CT with contrast agent 5 days post therapy

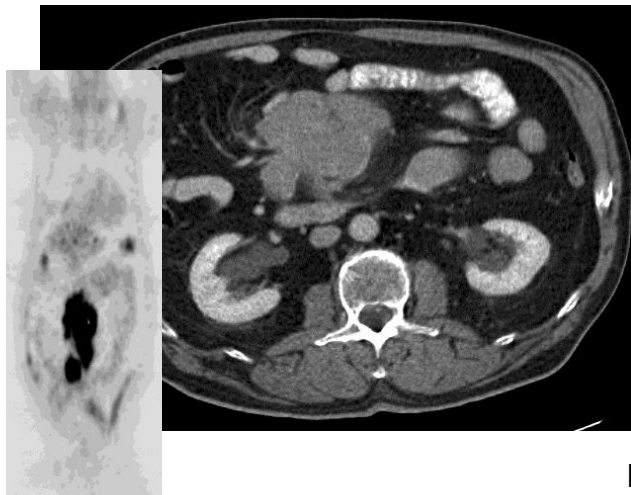




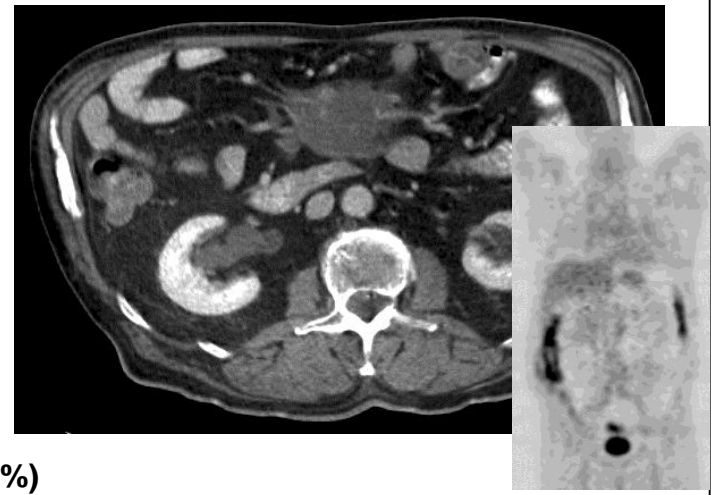
Patient 1



CRu (SPD – 84%)



Patient 2



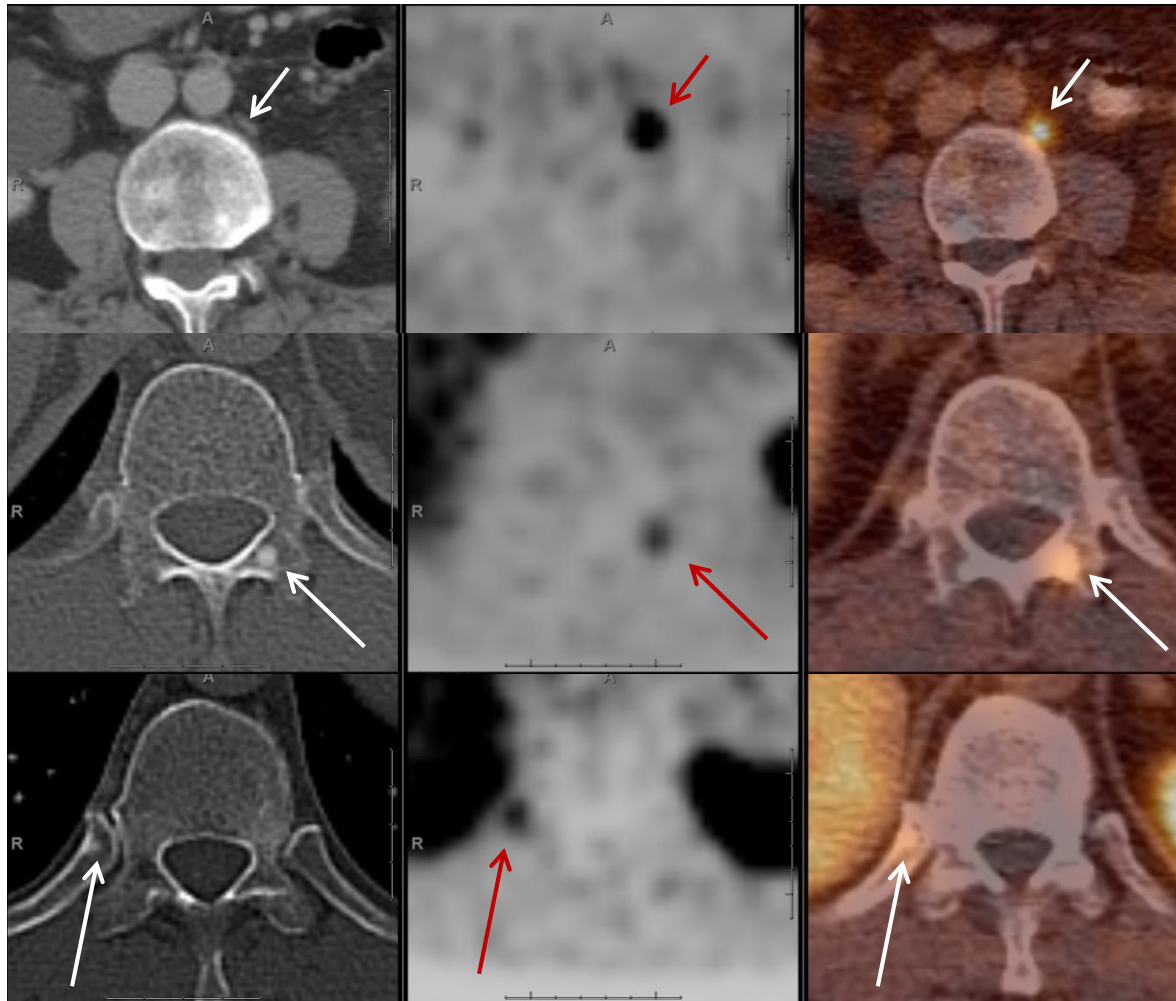
PR (SPD – 55%)

PSMA PET/CT

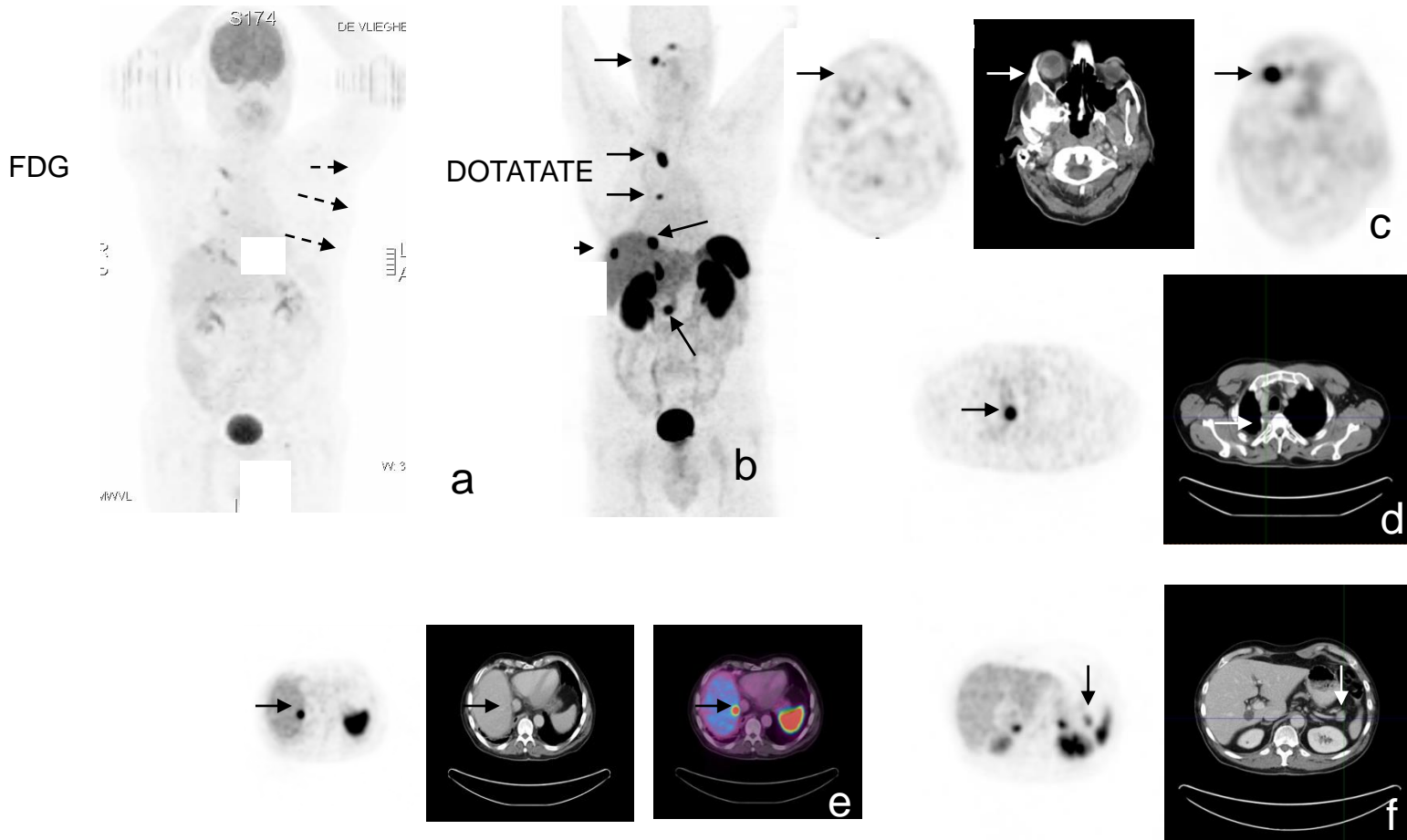
CT

PET

Fusion



Bronchial carcinoid with sudden onset of blurry vision



Small animal imaging

- Important for development of new tracer
- Final preclinical step in the process from bench to bedside

- μ SPECT / CT
- μ PET / CT

Small Animal Imaging / Model Examples



Small Animal -
PET/CT



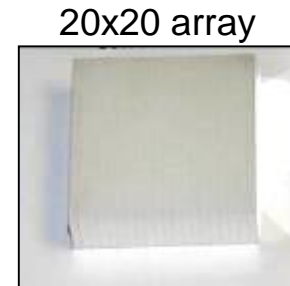
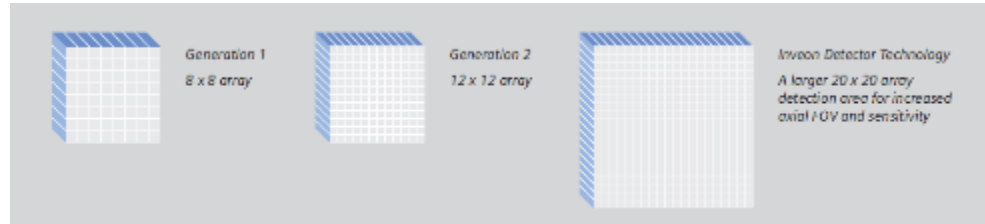
Small Animal –
SPECT/CT



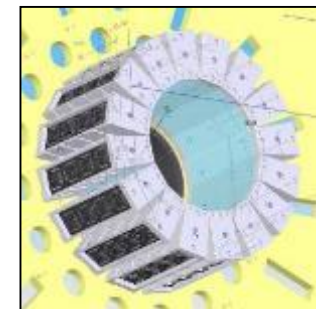
Small Animal –
PET/SPECT/CT

Micro PET: Dedicated Small Animal System

- Micro PET Siemens Inveon



- Detector diameter: 16,1 cm
- Transaxial FOV: 10,0 cm
- Axial FOV: 12,7 cm
- Crystal-detectors: LSO - 64 Blocks
25600 Sum of single crystals
- High resolution: 1,4 mm FWHM
- Absolut Sensitivity: 100,0 cps / 1kBq , 10 %



Micro PET: Dedicated Small Animal System

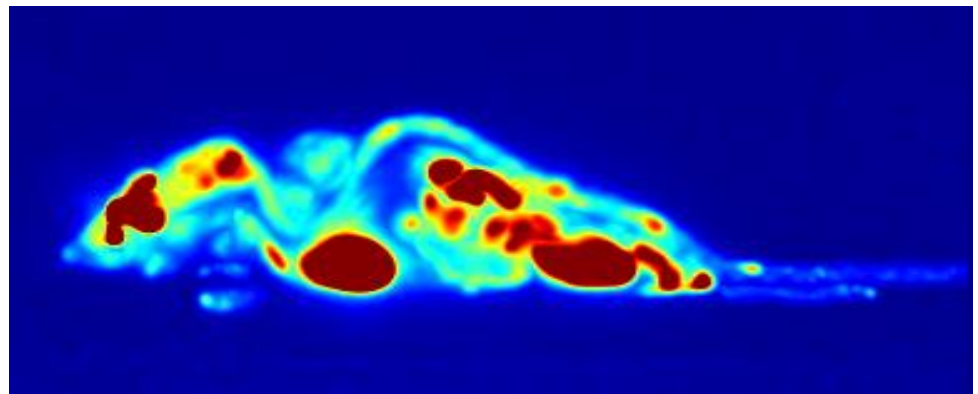
- Micro PET Siemens Inveon

Micro PET - measurement of the glucose metabolism with ^{18}F -FDG and of the skeleton with the bone affine radiopharmaceutical ^{18}F -NaF in a mouse.

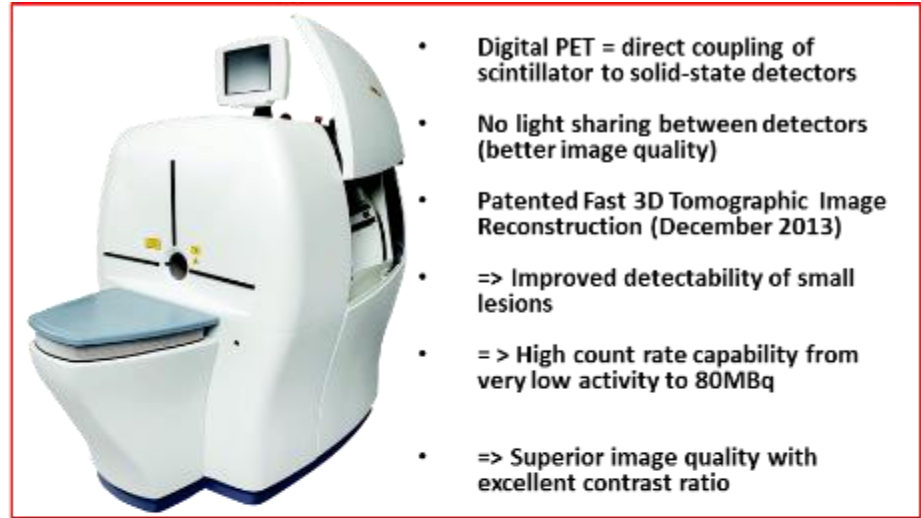
^{18}F -Sodium fluoride



^{18}F -Fluorodesoxyglucose



Digital PET Sub-System



- Digital PET = direct coupling of scintillator to solid-state detectors
- No light sharing between detectors (better image quality)
- Patented Fast 3D Tomographic Image Reconstruction (December 2013)
- => Improved detectability of small lesions
- => High count rate capability from very low activity to 80MBq
- => Superior image quality with excellent contrast ratio

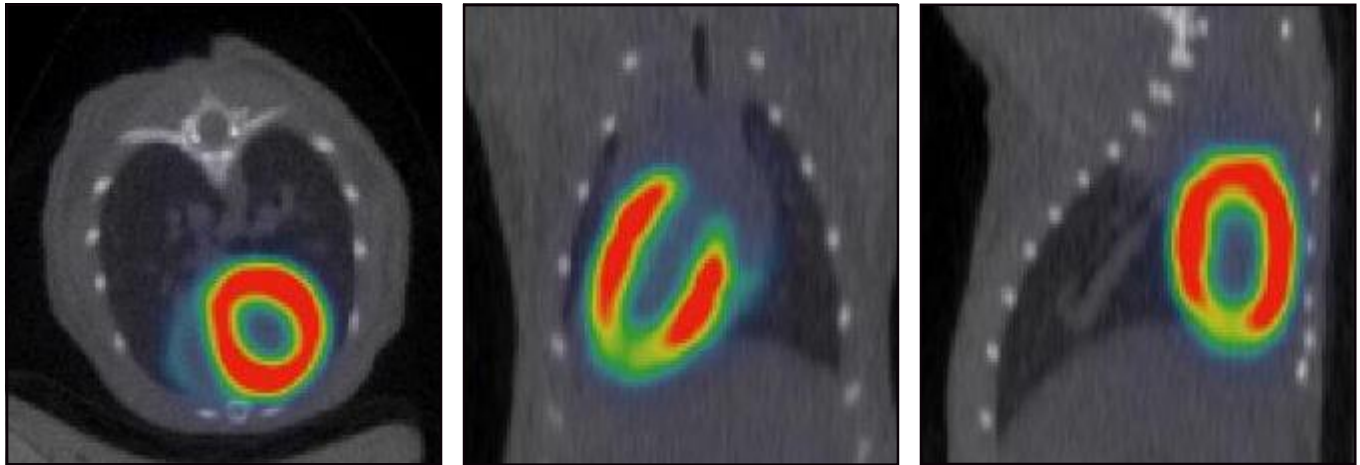
- ◆ Bore diameter: 15cm
- ◆ Transaxial FOV: User-selectable 46-100 mm
- ◆ Axial FOV: 30cm (continuous motion)
 - LabPET4
 - LabPET8
 - LabPET12

- Quad-APD detector modules coupled with LYSO/LGSO phaswich scintillators
- Individual readout, parallel signal processing
- Fully integrated with SPECT and CT;
- field- upgradable

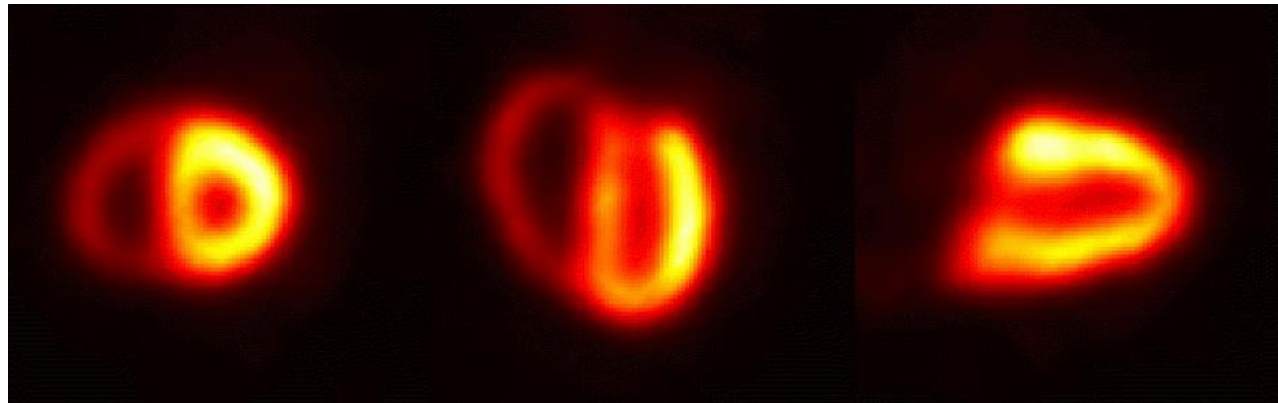
TriFoil

PET/CT Cardiac Imaging - Mouse

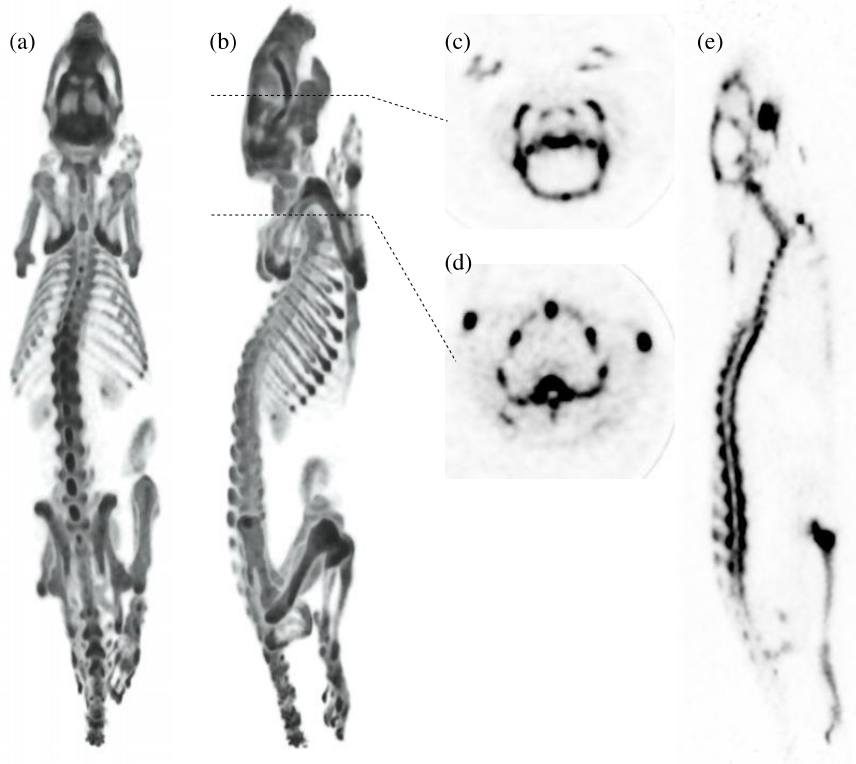
PET/CT:
0.7mCi of
FDG, 20min.
Post injection,
5 min. scan



Detail of gated
cardiac images



Courtesy of Dr. Ren-Shyan Liu, National Yangming University, Taipei, Taiwan



LabPET 8

Figure 10. Volume-rendered images (a), (b) of a 185 g rat injected with 31 MBq of Na^{18}F and scanned 68 min post-injection on the LabPET8. Transaxial slices of the skull (c) and the ribcage (d) and a sagittal slice (e) are shown. The whole-body image was obtained by acquiring five overlapping decay-compensated scans with 3.78 cm steps for a total of 60 min. The image was obtained with a lower energy threshold of 350 keV and reconstructed using 80 3D MLEM iterations.



Reference: Imaging performance of LabPET APD-based digital PET scanners for pre-clinical research; M. Bergeron et al.; Universite de Sherbrooke, QC, Canada; Phys. Med. Biol. 59 (2014) 1–18

Small Animal Imaging / Model Examples



Small Animal -SPECT/CT



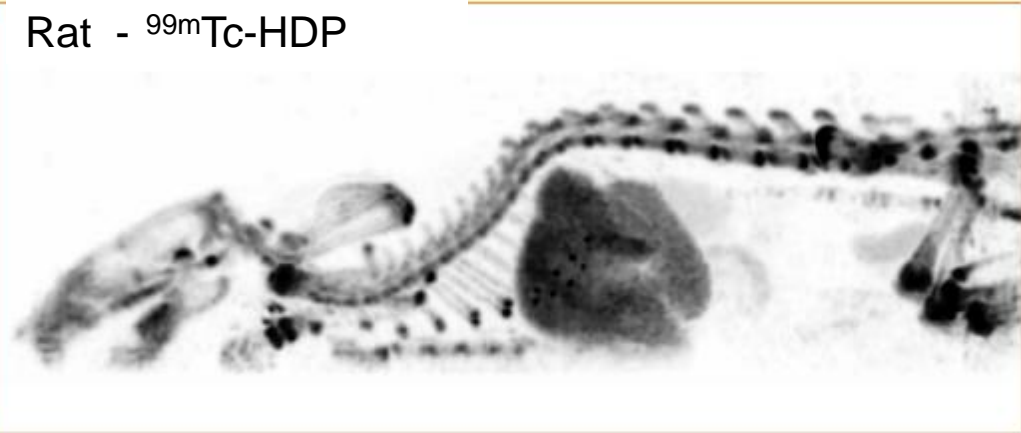
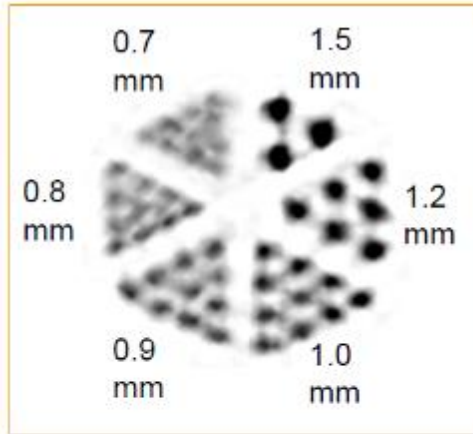
Small Animal -SPECT/CT

MMP - S P E C T

- Micro SPECT: Measurement of the bone skeleton with ^{99m}Tc -HDP

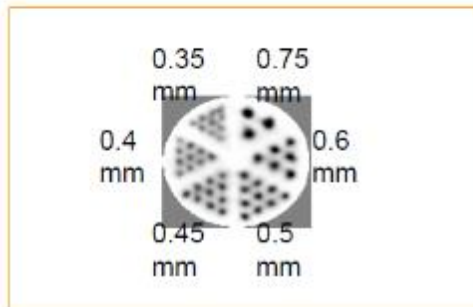
Rat collimator

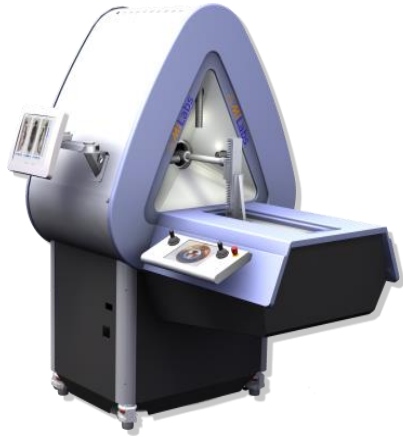
Rat - ^{99m}Tc -HDP



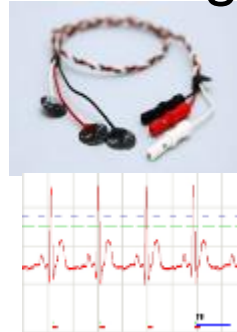
Mouse collimator

Mouse - ^{99m}Tc -HDP

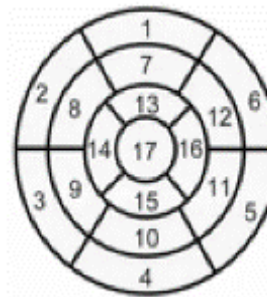
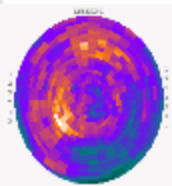
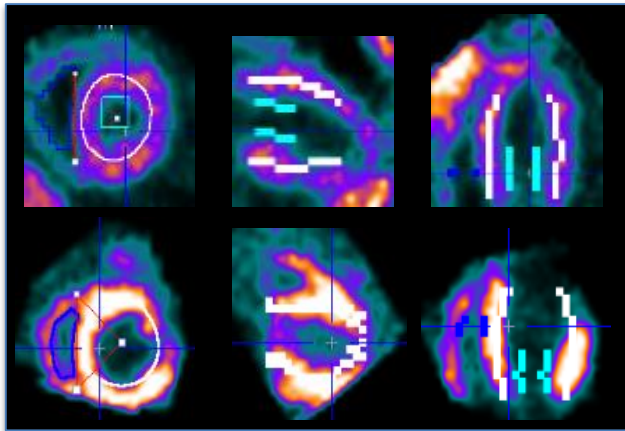




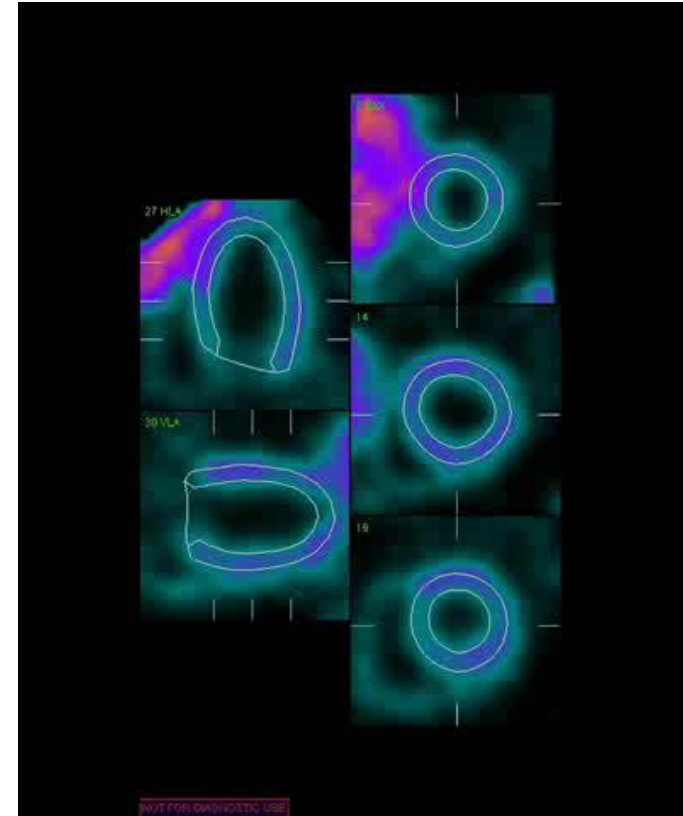
ECG gating



CARDIAC PMOD – 17 segment model



- | | | |
|------------------------|-----------------------|---------------------|
| 1. basal anterior | 7. mid-anterior | 13. apical anterior |
| 2. basal anteroseptal | 8. mid-anteroseptal | 14. apical septal |
| 3. basal inferoseptal | 9. mid-inferoseptal | 15. apical inferior |
| 4. basal inferior | 10. mid-inferior | 16. lateral |
| 5. basal inferolateral | 11. mid-inferolateral | 17. apex |
| 6. basal anterolateral | 12. mid-arterolateral | |

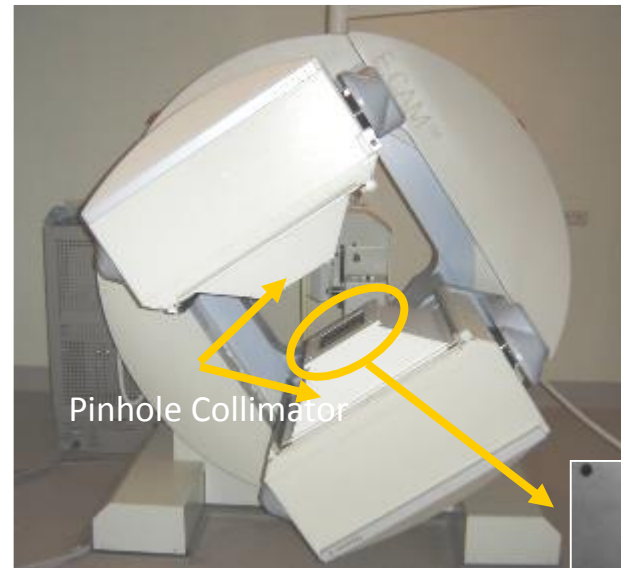
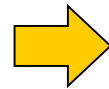


Multiplex Multi Pinhole (MMP) - S P E C T

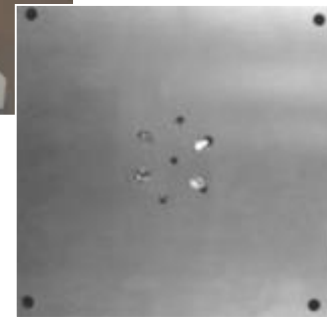
- Micro SPECT: MMP-Technology with a clinically used SPECT gamma camera
 - Physical measuring principals
 - Characterisation and performance parameters



Siemens SPECT E.cam gamma camera



7-Pinhole Aperture Plate



MMP - S P E C T

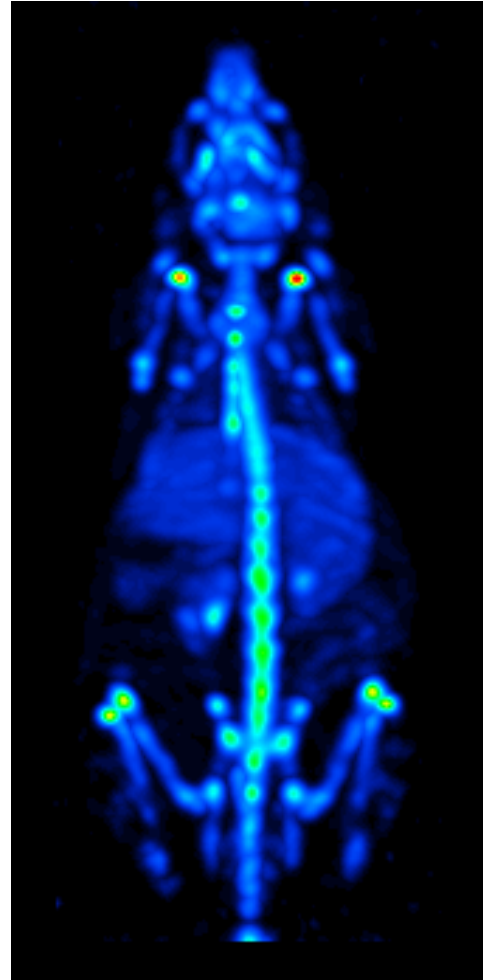


MMP - S P E C T

- Micro SPECT: Measurement with MMP-Technology by a clinically used SPECT gamma camera

● SPECT

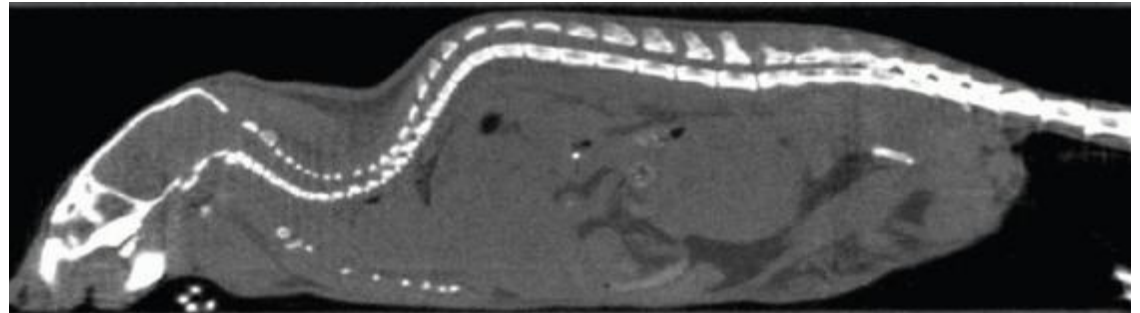
^{99m}Tc -HDP



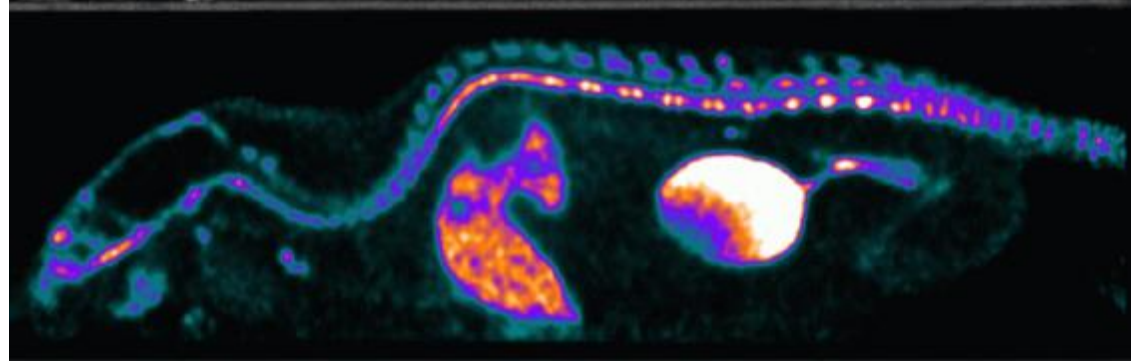
MMP - S P E C T

- **Micro SPECT:** Measurement of a mouse bone skeleton with ^{99m}Tc -HDP

CT

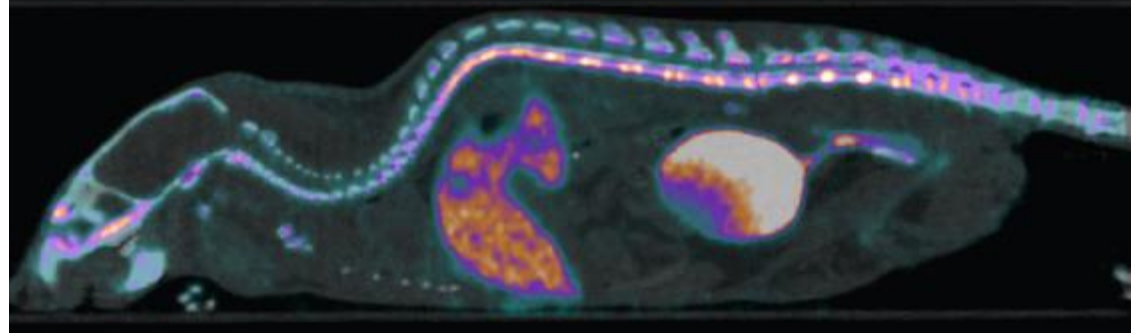


^{99m}Tc -Hydroxy-Diphosphonat



Fusion

CT - ^{99m}Tc -HDP SPECT



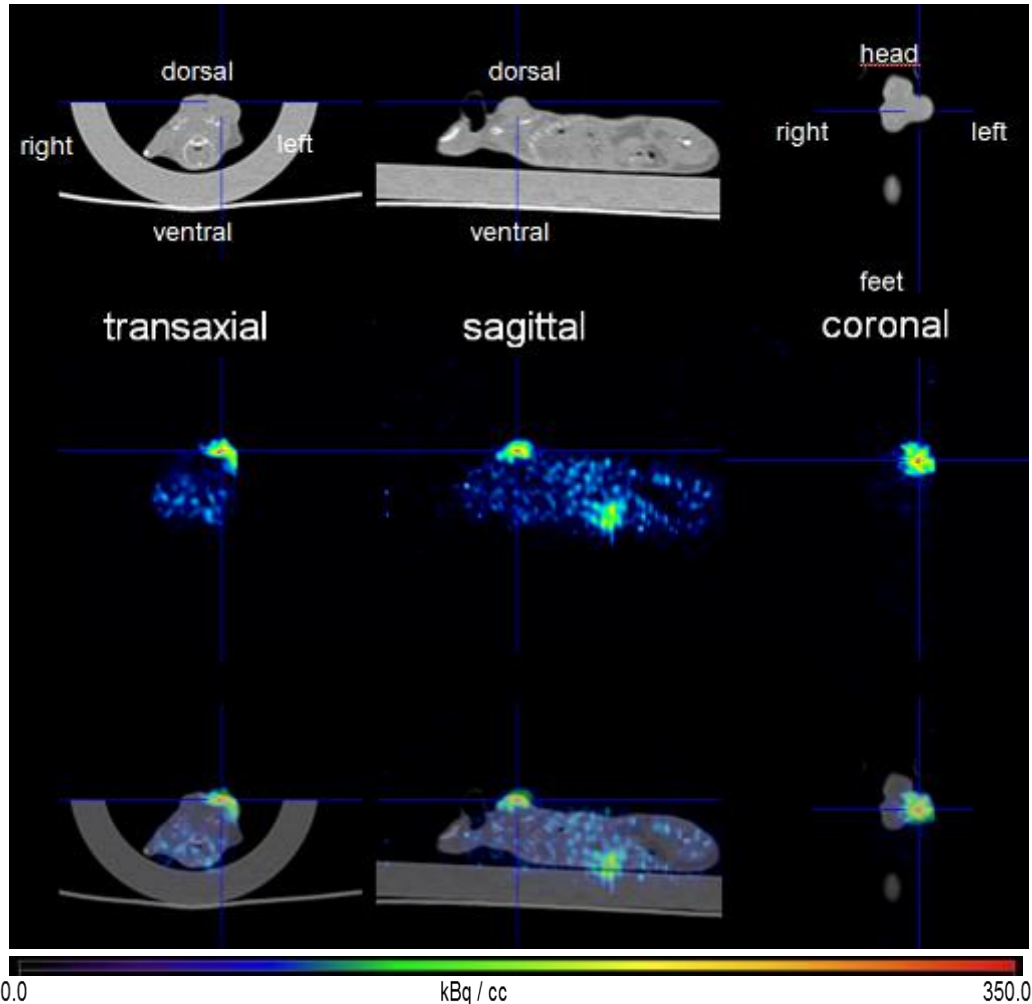
Biodistribution of ^{123}I -5-iodo-4'-thio-2'-deoxyuridine (^{123}I -ITdU) in WiDr xenografted mouse models - MMP μSPECT , 10.0 MBq 60 min p.i.

CT

**μSPECT [^{123}I]-ITdU
FdUrd-Appl.**

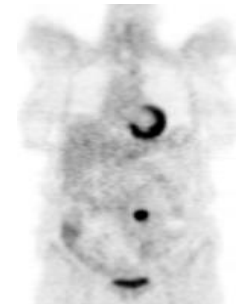
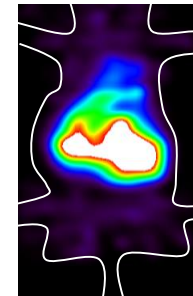
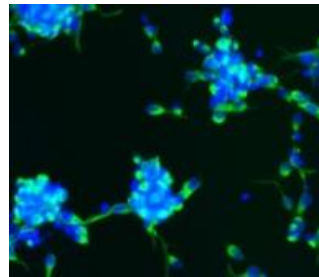
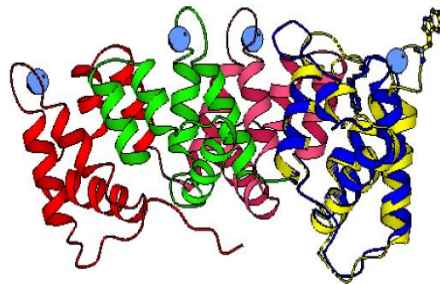
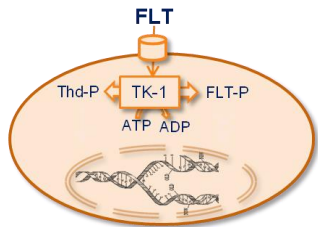
Fusion

**μSPECT [^{123}I]-ITdU
+ CT**



Examples for small animal imaging: biodistribution studies play a major role

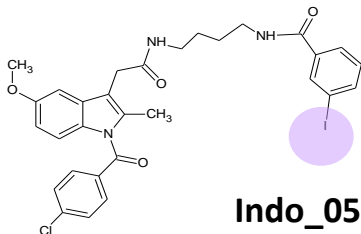
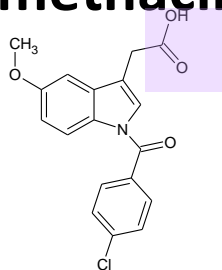
- **New tracer development**
- **New pharmaca development**
- **Therapy studies**



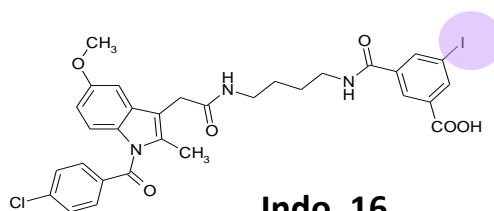
Indomethacin derivatives targeting COX2

Indomethacin as chemical lead

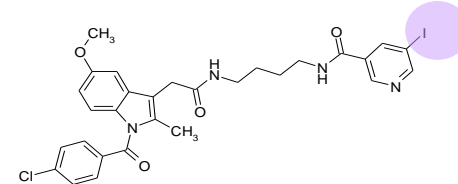
Derivatization at carbonic acid \Rightarrow Indometacin-Derivate with different Polarity and charge for labeling with radio iod und radio fluor



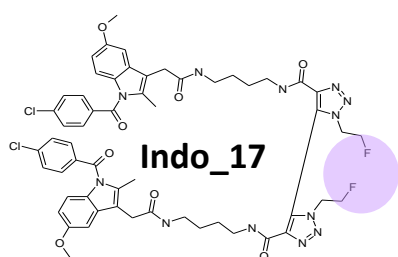
Indo_05



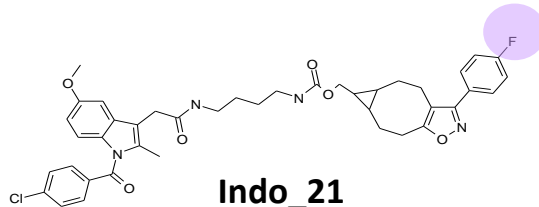
Indo_16



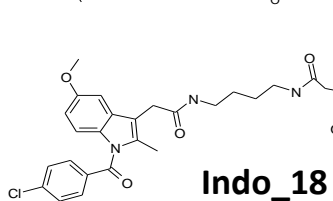
Indo_23



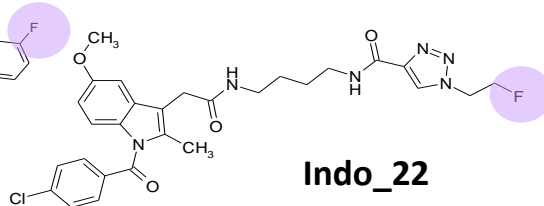
Indo_17



Indo_21



Indo_18



Indo_22

Cite this: *Chem. Commun.*, 2012, 48, 7134–7136

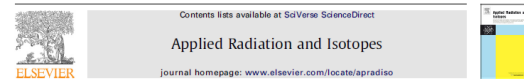
www.rsc.org/chemcomm

COMMUNICATION

Beyond azide–alkyne click reaction: easy access to ^{18}F -labelled compounds *via* nitrile oxide cycloadditions†

Boris D. Zlatopolskiy,^{a,b} René Kandler,^b Diana Kobus,^b Felix M. Mottaghy^{a,c} and Bernd Neumaier^{a,b}

Applied Radiation and Isotopes 70 (2012) 184–192



C-(4-[^{18}F]fluorophenyl)-N-phenyl nitrene: A novel ^{18}F -labeled building block for metal free [3+2]cycloaddition

Boris D. Zlatopolskiy^{a,b}, René Kandler^a, Felix M. Mottaghy^{b,c}, Bernd Neumaier^{a,*}

^aMax Planck Institute for Neurological Research, Gendler Straße 50, 50931 Cologne, Germany

^bKlinik für Nuklearmedizin, Aachen University, RWTH, Pauwelsstr. 30, 52074 Aachen, Germany

^cDepartment of Nuclear Medicine, Maastricht University Medical Center, P. Debyeaan 25, 6201BX Maastricht, the Netherlands

PET [18F]FLT

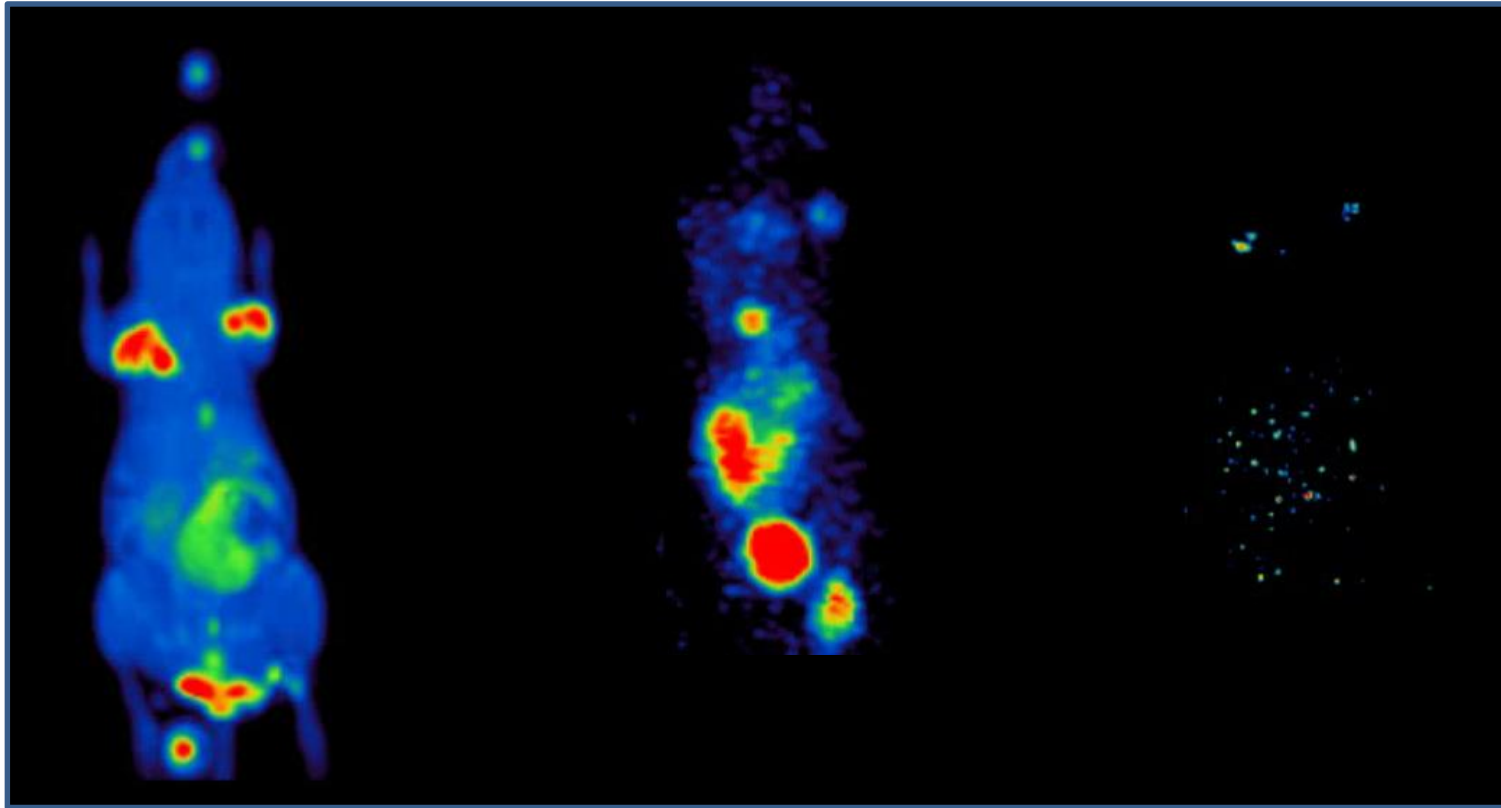
FdUrd-Appl.

μ SPECT [123I]-ITdU

FdUrd-Appl. 60 min p.i.

μ SPECT [123I]-ITdU

FdUrd-Appl. 24 h p.i.



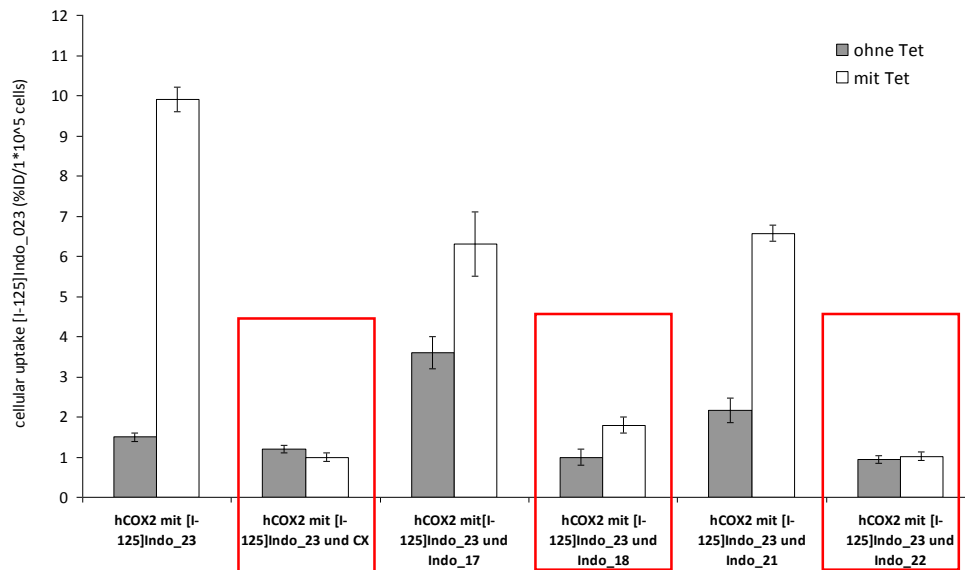
0.0

kBq / cc

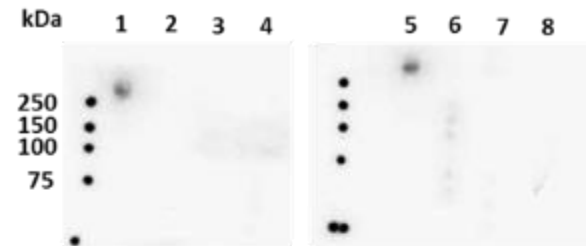
830.0

COX2-specific Inhibitors: PET-Tracer

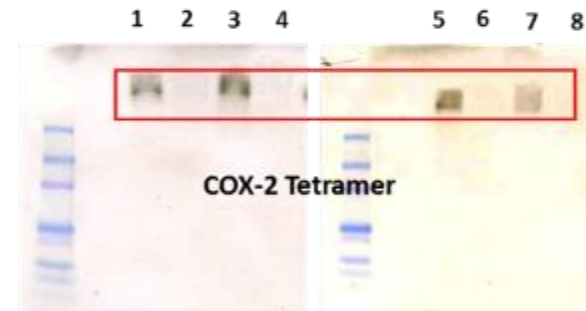
Cellular uptake of COX2-PET Tracer: Competition study with cold standards and [125 I]Indo_23 as COX2 Tracer und corresponding PhosphorImager and Western Blot Analysis



PhosphorImager Analysis



Western Blot Analyse with COX2-spec. Ab



1. HEK COX-2 mit [125 I]Indo_23, Tet stimulated
2. HEK COX-2 [125 I]Indo_23, unstimulated
3. HEK COX-2 mit [125 I]Indo_23 + CX, Tet stimulated
4. HEK COX-2 mit [125 I]Indo_23 + CX, unstimulated
5. HEK COX-2 mit [125 I]Indo_23 + Indo_21, Tet stimulated
6. HEK COX-2 mit [125 I]Indo_23 + Indo_21 unstimulated
7. HEK COX-2 mit [125 I]Indo_23 + Indo_22, Tet stimulated
8. HEK COX-2 mit [125 I]Indo_23 + Indo_22, unstimulated

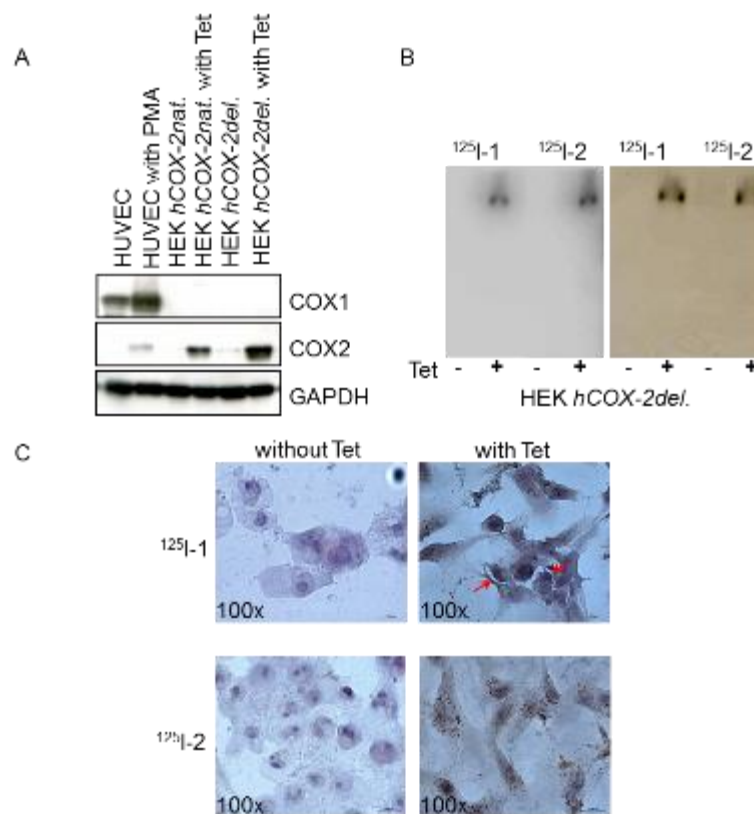


Fig. 3. Binding specificity and intracellular distribution of iodinated indomethacin derivatives. (A) SDS and western blot analysis of COX-1 and COX-2 expression in HUVEC, HEK hCOX-2nat and HEK hCOX-2del cells in dependency on PMA- and Tet-stimulation, respectively. GAPDH served as a loading control. (B) SDS gel electrophoresis of cell lysates obtained from HEK hCOX-2del cells incubated with ¹²⁵I-1 and ¹²⁵I-2 and visualized by phosphorimager (*left*); subsequent western blot analysis with COX-2 specific antibody. (C) Intracellular localization of ¹²⁵I-1 and ¹²⁵I-2 in HEK hCOX-2del cells detected by microautoradiography followed by a standard H&E staining.

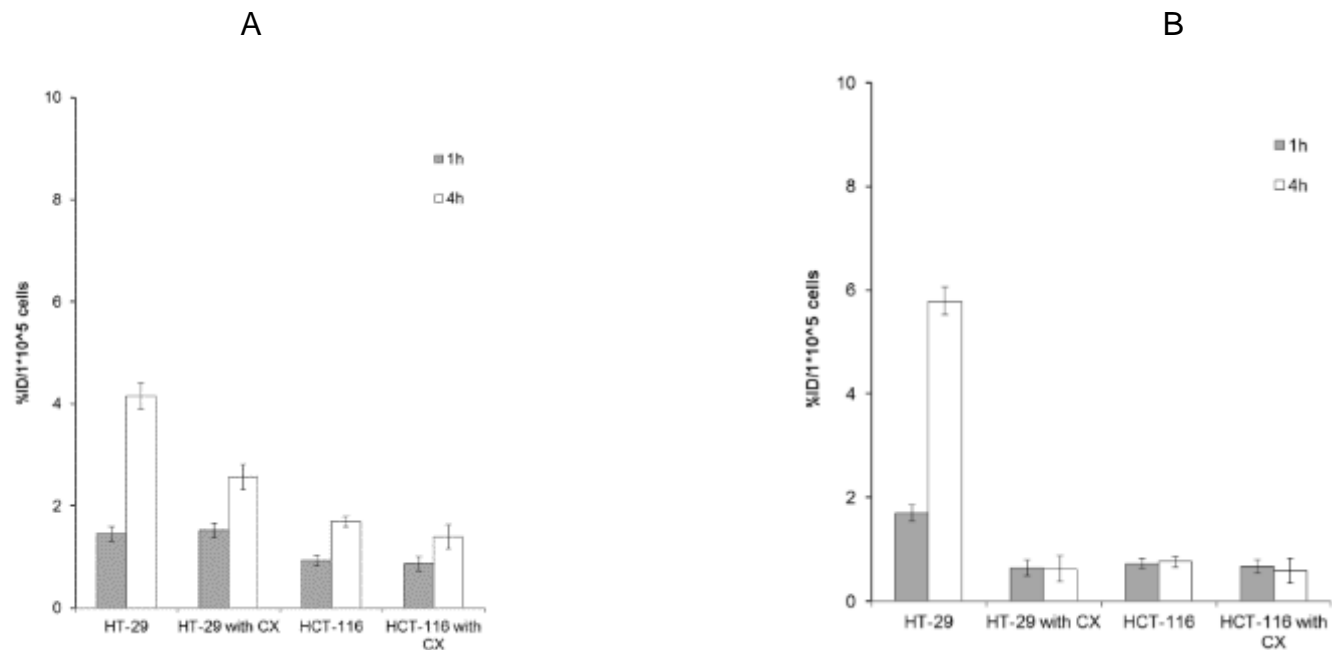


Fig. 4. Cellular uptake with ¹²⁵I-1 and ¹²⁵I-2 compounds in colon carcinoma cells after 1h and 4h incubation (in % of incubated dose (ID)/well). (A) Cellular uptake of ¹²⁵I-1 in HT29 and HCT-116 cells w/o and with CX. (B) Cellular uptake of ¹²⁵I-2 in HT29 and HCT-116 cells w/o and with CX.

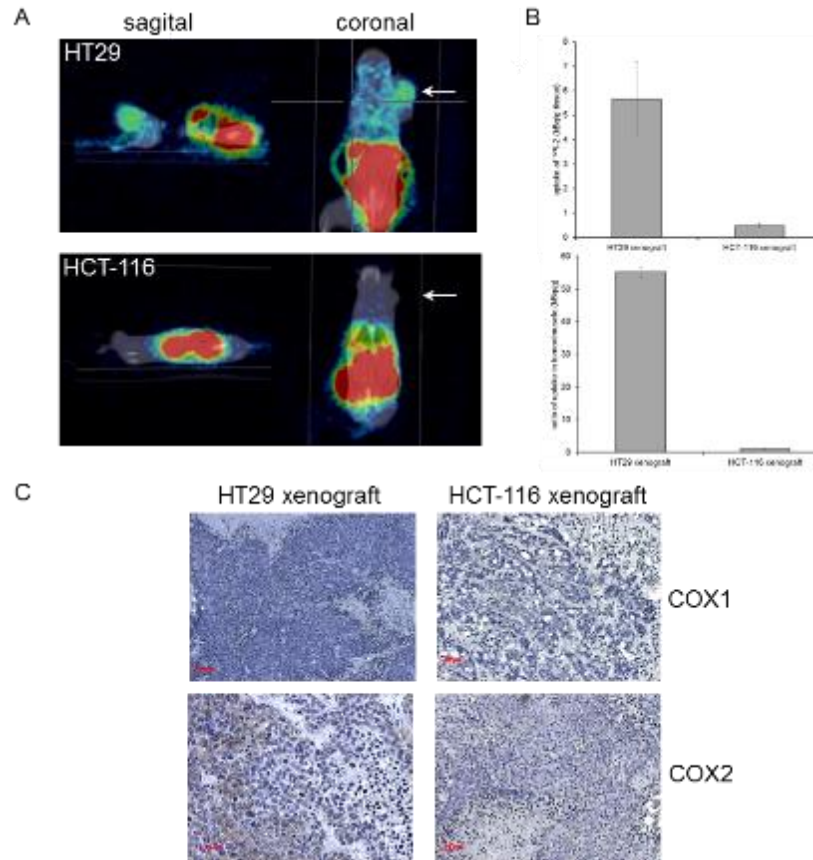
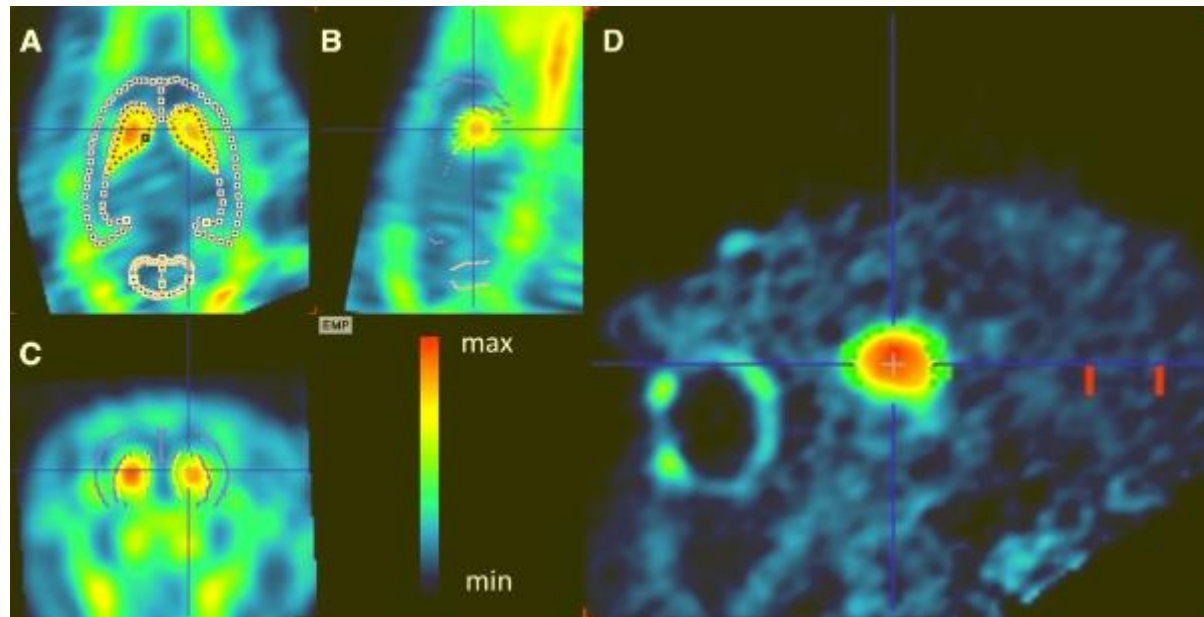
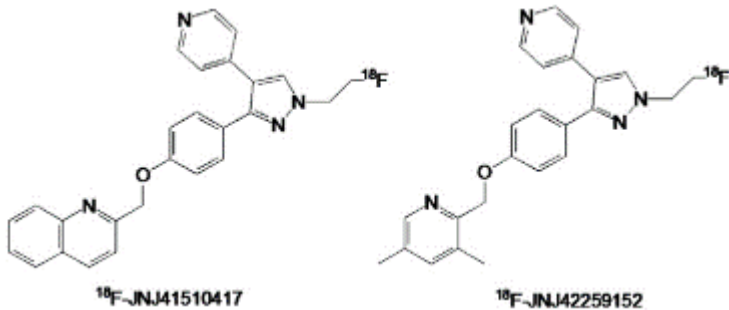
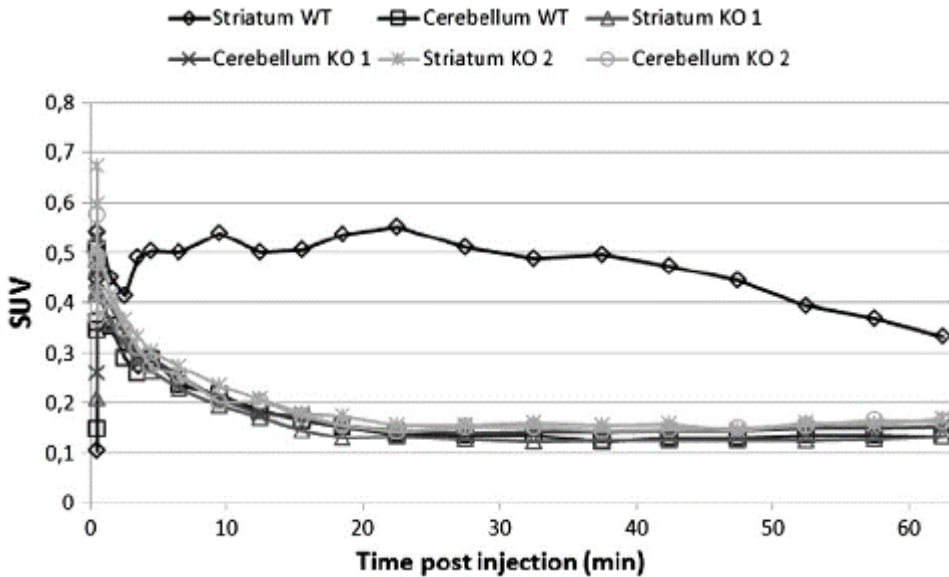


Fig. 5. *In vivo* study with ^{124}I -2 compound in colon carcinoma xenografted SCID mice. (A) $\mu\text{PET}/\text{CT}$ molecular imaging of COX-2 with ^{124}I -1 in HT29 (upper panel) and HCT-116 (lower panel) xenografted SCID mice at 4h p.i.. (B) Uptake of ^{125}I -2 in HT29 and HCT-116 tumors (in kBq/g tissue) (upper panel); tumor to muscle uptake ratio of ^{125}I -2 in HT29 and HCT-116 tumor xenografted mice (lower panel). (C) immunohistological analysis of COX-1 and COX-2 in HT29 and HCT-116 xenografts.

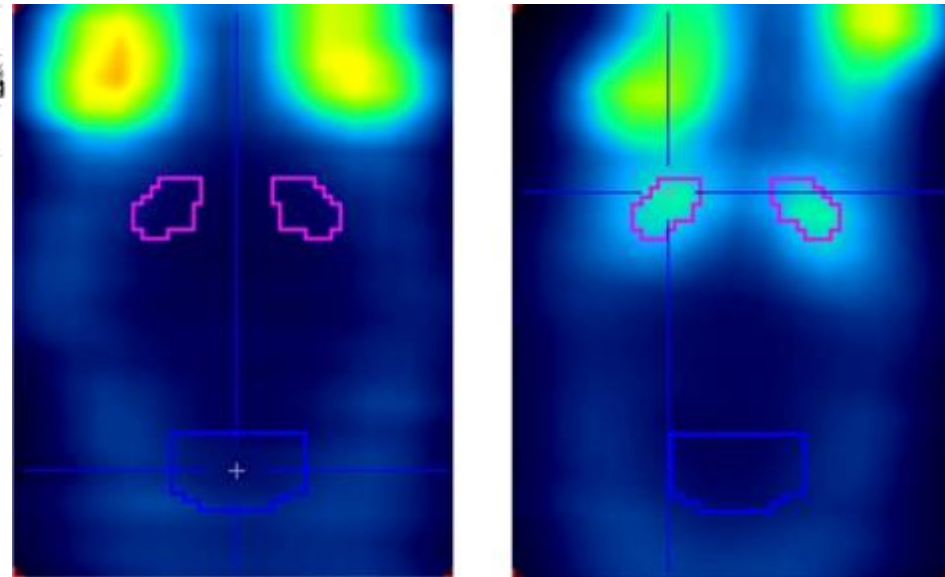
New pharmaca development

Phosphodiesterase-10A (PDE10A) is implicated in several neuropsychiatric disorders involving basal ganglia neurotransmission, such as schizophrenia, obsessive–compulsive disorder and Huntington's disease.



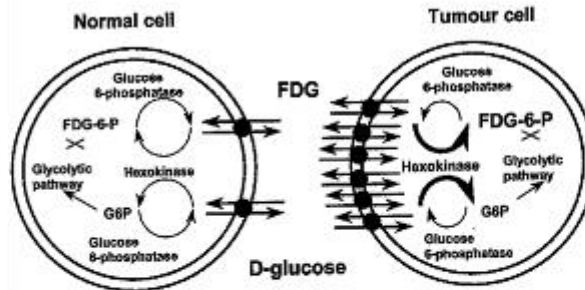


Small-animal PET transversal sections of KO (left image) and WT (right image) mouse brain injected with $[^{18}\text{F}]\text{JNJ42259152}$ (summed images from 0 to 60 min post tracer injection). ROIs were drawn on the areas corresponding to striatum and cerebellum to obtain the TACs of $[^{18}\text{F}]\text{JNJ42259152}$ in striatum and cerebellum of two PDE10A KO mice and one WT mouse (WT = wild type mouse, KO = PDE10A knock-out mouse).



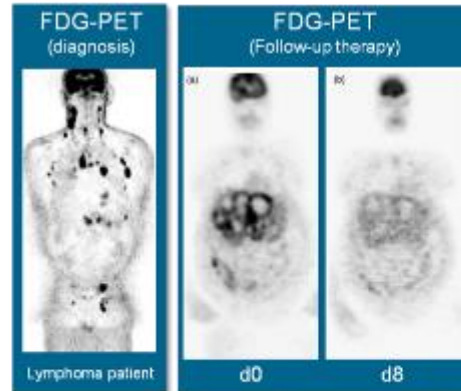
Glucose metabolism: therapy response

¹⁸F-FDG – PET



Eur J Nucl Med Mol Imaging (2010) 37:1688–1695
DOI 10.1007/s00259-010-1479-0

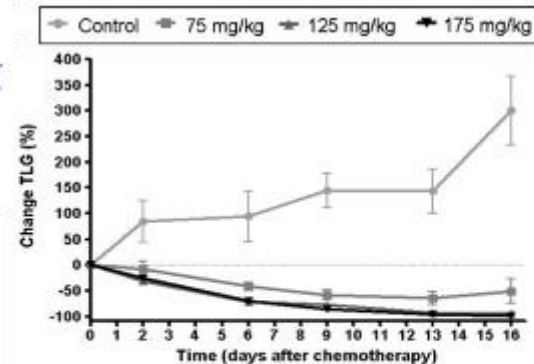
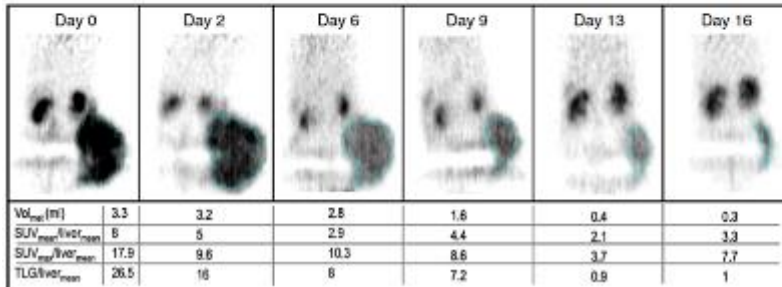
ORIGINAL ARTICLE



Stroobants et al., E J Cancer 2003

Dose-response relationship in cyclophosphamide-treated B-cell lymphoma xenografts monitored with [¹⁸F]FDG PET

Lieslot Brepoels · Marijke De Saint-Hubert ·
Sigrid Stroobants · Gregor Verhoef · Jan Balzarini ·
Luc Mortelmans · Felix M. Mottaghy



→ [¹⁸F]FDG –Uptake represents dose-effect-dependency of Cyclophosphamid

Proliferation: Therapy Response

¹⁸F-FLT – PET

Am J Nucl Med Mol Imaging 2012;2(1):110-121
[www.ajnmj.us/ISSN:2160-8407/ajnmj1111001](http://www.ajnmj.us/)

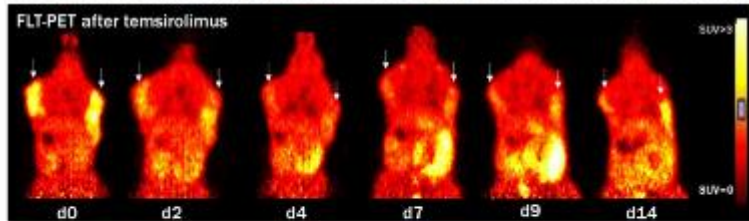
Original Article

Molecular imaging of therapy response with ¹⁸F-FLT and ¹⁸F-FDG following cyclophosphamide and mTOR inhibition

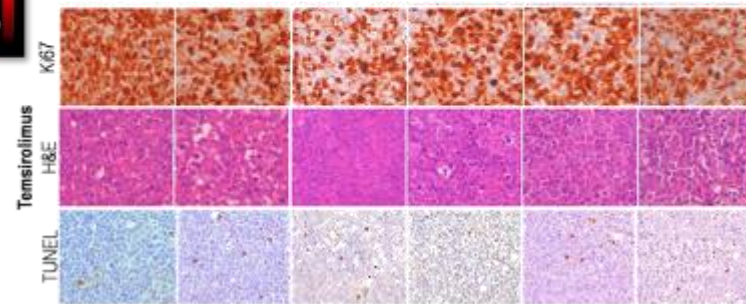
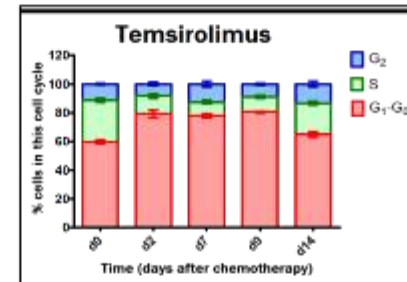
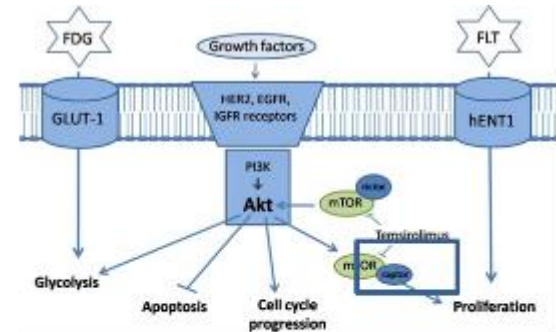
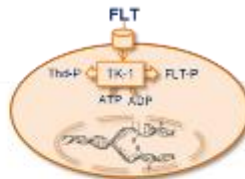
Marjke De Saint-Hubert¹, Lieselot Brepoels², Ellen Devos³, Peter Vermaelen³, Tjibbe De Groot³, Thomas Tousseyn⁴, Luc Mortelmans², Felix M Mottaghy^{1,2,5}

¹Department of Nuclear Medicine, Maastricht University Medical Centre, Maastricht, The Netherlands; ²Department of Nuclear Medicine, Katholieke Universiteit Leuven, Leuven, Belgium; ³Laboratory for Radiopharmacy, Katholieke Universiteit Leuven, Leuven, Belgium; ⁴Morphology and Molecular Pathology, Katholieke Universiteit Leuven, Leuven, Belgium; ⁵Department of Nuclear Medicine, University Hospital RWTH Aachen, Germany

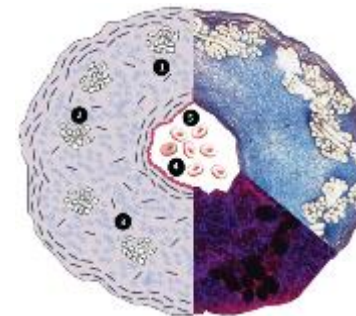
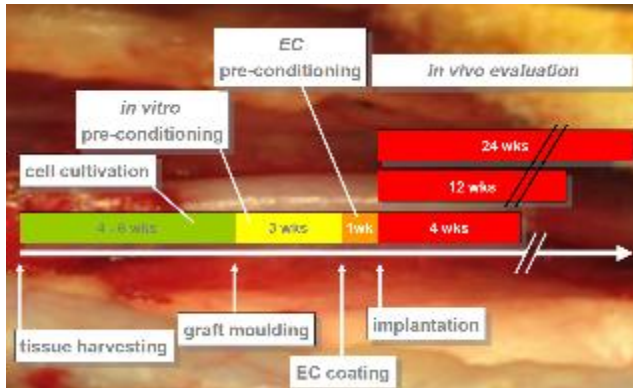
Received November 5, 2011; accepted November 18, 2011; Epub December 15, 2011; Published January 1, 2012



- FLT-PET represents reduced proliferation after temsirolimus.
- Correlates with the end of mitosis (Increase of G₀/G₁ in Facs) and ki67- staining



- **SPECT and PET**
 - provide a broad spectrum of diagnostic approaches
 - help to understand biological processes
 - are an important link in the „bench to bedside“ concept of probe development
- **Molecular Imaging**
 - is important for non-invasive monitoring of disease
 - supports development of new theranostic concepts



J. Frese et al.: Monitoring of tissue engineered constructs